People's Democratic Republic of Algeria

Ministry of Higher Education and Scientific Research

University of Tebessa

Faculty of Science and Technology

Department of Mechanical Engineering

Ref: 2019/2020

MASTER'S DISSERTATION

Option:

Materials Engineering

Theme

Elaboration and Characterization of Nickel Oxide thin films doped Cobalt

Presented by:

DRID Badreddine

Publicly defended on: 29/06/2020

In front of the jury committee composed of:

LAOUADI Bouzid	MCB	Tebessa University	President
DIHA Abdallah	MCA	Tebessa University	Supervisor
BOULEDROUA Basma	MAA	Tebessa University	Examiner

University year: 2019 / 2020


بِسْمِ اللَّهِ الرَّحْمَٰنِ الرَّحِيمِ ﴿١﴾
الْحَمْدُ لِلَّهِ رَبِّ الْعَالَمِينَ ﴿٢﴾ الرَّحْمَٰنِ الرَّحِيمِ ﴿٣﴾
مَالِكِ يَوْمِ الدِّينِ ﴿٤﴾ إِيَّاكَ نَعْبُدُ
وَإِيَّاكَ نَسْتَعِينُ ﴿٥﴾ اهْدِنَا الصِّرَاطَ
الْمُسْتَقِيمَ ﴿٦﴾ صِرَاطَ الَّذِينَ أَنْعَمْتَ عَلَيْهِمْ
غَيْرِ الْمَغْضُوبِ عَلَيْهِمْ وَلَا الضَّالِّينَ ﴿٧﴾

Dedication

All Thanks to:

1st to Allah

2nd to My Parents

3rd to MY Supervisor

4th to My Brother

5th to My Cousin

" My Brother from Another Mother "

Badreddine Drid


Contents

Contents

Chapter 2: Elaboration and Characterizations of NiO: Co Thin Films

Chapter 3: Results and Discussion

List of Figures

List of Tables

List of Symbols

Symbol	Meaning	Unit
W	The mass	G
I	The current	A
E	The chemical equivalent weight	G
T	The time	S
F	constant called the Faraday	-
m	Mass Molar	G
M	Molar mass	Mol
C	The concentration	mol/l
V	The volume	L
A	The expansion coefficients	K^{-1}
P	The pressure	Bar
$\mathbf{d_{hkl}}$	Inter-planner Spacing	Å
hkl	the miller indices	-
Θ	Diffraction Angle	Degree
$\mathbf{a^2}$	Atomic distance	Nm
$\mathbf{D_{hkl}}$	The average grain size	-
$\boldsymbol{\beta_{hkl}}$	The full width at half maximum intensity	-
$\mathbf{T_C}$	Texture Coefficient	-
N	Reflection number	-
E	The strain	-
$\mathbf{a_o}$	Lattice Constant	Å
Δ	Dislocation Density	cm^{-2}
$\mathbf{D_{av}}$	The Crystallite Size	Nm
T	The thickness	Nm
$\mathbf{N_0}$	The number of crystallites	cm^{-2}
$\mathbf{I_o}$	Incident intensity	mW/cm^2
$\mathbf{I_A}$	Absorbed light intensity	mW/cm^2
T	Transmittance	-
A	Absorbance	-
$\mathbf{E_g}$	Energy Band gap	Ev
$\mathbf{E_u}$	Urbach energy	MeV

Λ	Wavelength of Incident Light	Nm
hv	Photon Energy	Ev
R_s	Sheet resistance	Ω/square
R_b	The bulk resistivity	Ω/Cm
Δ_m	The weight difference	G
A_S	Area	Cm^2
ρ_0	The Density of Material	g/cm3

List of Acronyms

Symbol	Meaning
TCO	Transparent Conductive Oxides
TBL	Thermal Barrier Layer
Ni	Nickel
NiO	Nickel Oxide
CO	Cobalt
F.C.C	Face-Centered Cubic
EUV	Evaporation Under Vacuum
CS	Cathode Sputtering
PLD	Pulsed Laser Deposition
TE	Thermal Evaporation
CBD	Chemical Bath Deposition
CVD	Chemical Vapor Deposition
SPT	Spray Pyrolysis Technique
XRD	X-Rays Diffraction
UVS	UV-visible Spectrophotometer
ASTM	American Standard for Testing of Materials
JCPDS	Joint Committee for Powder Diffraction Standards


INTRODUCTION

General introduction

Studies carried out on semiconductors based on transparent oxides and of high electrical conductivity have attracted the attention of many researchers because of their various applications in the microelectronics and optoelectronics [1], industrial, medical, military and energy, especially environmental ones. The discovery of OTC dates back to the early twentieth century, when Bädeker found that the thin layers of Cadmium Oxide (CdO) deposited inside a luminescent discharge chamber were both conductive and transparent [2]. This first observation gave birth to a new research which remains a topical subject after a century. Obtaining such materials, presenting a good compromise between transparency in visible light and good electrical conductivity, constitutes an important industrial challenge. This materials, made of metallic oxides deposited in thin layers such as Cadmium Oxide (CdO), Indium Oxide (InO), Nickel Oxide (NiO) and Zinc Oxide (ZnO) have been known for a long time. The layers of 100-200 Å thickness which are based on elements like CO, Au, Ag, Cu and Fe… etc. also have similar physical properties but are, in general, unstable over time and undergo degradation. The surface coatings with semiconductor materials find wide fields of application, because of their stability and hardness which are clearly superior to those of metallic layers [3].

In this work, thin layers of Nickel Oxide (NiO) and Cobalt doped nickel oxide (NiO: CO) prepared with different concentrations of the solution (0.015M, 0.030M, 0.045M, 0.060M, 0.075M) are produced using a solution Nickel Nitrate and Cobalt Chloride as a precursor to prepare good quality and homogeneity thin films on glass substrates by chemical spray pyrolysis technique (SPT) at temperature of (450 ±30 °C). The work was carried out at the Laboratory of Materials Engineer at the University of Tebessa.

The main objective of this work is study the effect of Cobalt doping Nickel Oxide on : structural, optical and electrical characteristics using different characterization techniques such as : X-ray diffraction for micro-structural characterization, UV-visible spectroscopy for optical characterization, four-point technique for electrical measurements and weight difference method for thickness measurement.

This thesis is structured in three chapters and General Conclusions as follows:

This dissertation started with a general introduction. The first chapter has exposed a brief bibliographical study on thin films in general and the nickel oxide in particular.

This study was followed by presenting its crystallographic, optical, electrical and chemical properties. The nickel oxide was used related of its remarkable properties and its multitude applications. Then this study was completed by presenting some propriety of Cobalt. At the end, we will provide description of various deposition methods of thin layers. We are focused on the spray pyrolysis method used in the present work, ending by some of advantages of this method.

The second chapter contained two parts which have consisted respectively detailed explanation of the different steps of preparation for our thin layers and characterization techniques used in this work.

In third chapter, we have presented our findings with some explanations and comparison

With previous works documented in literature where necessary.

Finally, conclusion summery of main results obtained, concluding and compared with the other previous works in the same field.


Chapter 1

I.1 Introduction

This first chapter includes general description of thin film, presentation of our premier materials, their propriety and some of their applications in different fields. In the end of this chapter we give some deposition methods.

I.2 General Information on thin films "NiO Case"

I.2.1 Definition of thin film:

It is possible to define a thin film of a material that is an element of this material so that its thickness is greatly reduced, which is expressed with nanometers (10^{-6} m). The small distance between the two boundary surfaces gives a disturbance of the physical, chemical and mechanical properties figure I.1.The essential difference between the material in the its bulk state and its the thin state is related to the fact that the role of the boundaries in the properties is usually neglected in the bulk state of materials, but in the thin state, on the contrary, the effects related to the boundaries are preponderant and very important [4] .It is quite obvious that the lower the thickness, the greater the bidimensionality effect. Conversely, when the thickness of a thin layer exceeds a certain threshold, the effect of thickness will become minimal and the material will return to the well-known properties of the solid state of material [5] .The second essential characteristic of a thin layer is that, whatever the procedure used for its manufacture, a thin layer is always integral with a substrate on which it is built (even if it sometimes happens that one separates the thin film of said substrate). Consequently, it will be imperative to take into account this major fact in the design, namely that the substrate has a very strong influence on the structural properties of the layer deposited therein. Thus a thin layer of the same material, of the same thickness may have substantially different physical properties depending on whether it will be deposited on an amorphous insulating substrate such as glass, or a monocrystalline silicon substrate .The purpose of the thin layer is to give particular properties to the surface of the part while benefiting from the massive properties of the substrate (in general: mechanical resistance), for example:

* **Electrical conductivity**: metallization of the surface, for example to observe an insulating sample under a scanning electron microscope.

* **Optical**: mirror glass, anti-reflective treatment of camera lenses, nickel plating of fire helmets to reflect heat (infrared), gilding of their visor to avoid glare.

I.2.2 Principle of deposit of thin films:

To form a thin layer on a solid surface (substrate) the particles of the coating material must pass through a conductive medium until intimate contact with the substrate. When the substrate arrives, a fraction of the coating particle adheres or reacts chemically with the substrate. The particles can be atoms, molecules, ions or fragments of ionized molecules. The transport medium can be solid, liquid, gas, or vacuum:

- a) **Solid**: in this situation, the substrate is in contact with the solid, only the particles which diffuse from the solid towards the substrate form a layer. Often, it is very difficult to obtain thin films by contact between solids, for example: the diffusion of Oxygen from Silica to form a thin SiO_2 layer on a Silicon substrate.
- b) **Liquid medium**: it is easier to use than the first case, because the material is more versatile in this state (epitaxy in liquid phase, and electrochemical, sol gel…).
- c) **Gas or vacuum**: this is a CVD type deposit where the difference between the gaseous medium and the vacuum is the average free path of the particles. There is no standard thin film deposition method that can be used in different situations. Substrate preparation is often a very important step for thin layer deposits in order to obtain good adhesion [6].

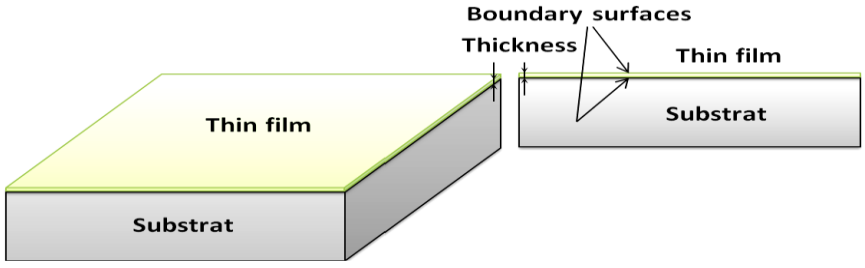

Figure I.1: Schematic of thin film deposited on a glass substrate [6].

I.2.3 Formation of thin films:

The process of depositing a thin layer is carried out in three stages [7]:

- ✓ Synthesis or creation of the species to be deposited.
- ✓ Transport of these species from the source to the substrate.
- ✓ Deposition on the substrate and growth of the layer.

Depending on the process followed, these steps can be completely separate from each other or else superimposed. Figure I.2 illustrates, in general, the process steps involved in the development
of thin layers
[8].

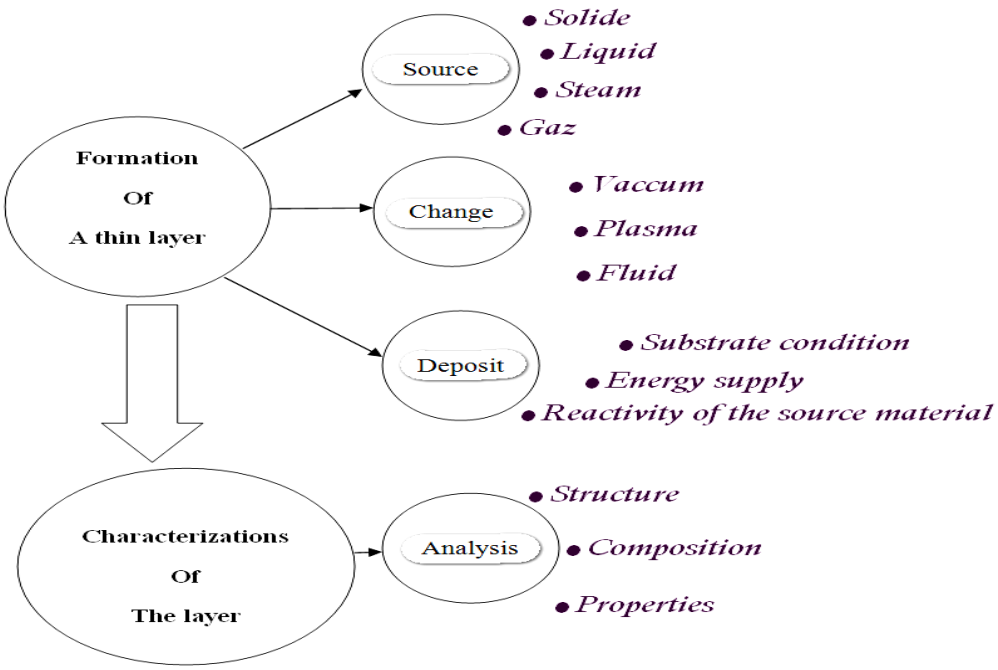

Figure I.2: Diagram of the steps of the thin film manufacturing process [8].

I.2.4 Interest and characteristics of thin films:

The interest of thin layers comes mainly from the economical use of materials in relation to the physical properties and the simplicity of the technologies used for their realization. A wide variety of materials are used to produce these thin layers. By putting them, we cite metals, alloys, refractory compounds (Oxides, Nitrides, and Carbides), intermetallic compounds and polymers.

The essential characteristic of a thin layer, whatever the procedure used for its manufacture, is that it is always integral with a support on which it is built (even if it sometimes happens that we separate the thin film of said support) . Consequently, it will be imperative to take this major fact into account in the design, namely that the support very strongly influences the structural properties of the layer which is deposited there.

Thus, a thin layer of the same material, of the same thickness, may have substantially different physical properties depending on whether it is deposited on an amorphous insulating

substrate such as glass or a monocrystalline Silicon substrate for example. It follows from these two essential characteristics of a thin layer the following consequence:

A thin layer is anisotropic by construction. In practice, we can distinguish two main families of thin layer production methods, those which use a carrier gas to move the material to be deposited from a container to the substrate and which are similar to the diffusion techniques used in the manufacture of active components, and those which involve an environment at very reduced pressure and in which the material to be deposited will be conveyed thanks to an initial pulse of thermal or mechanical nature [9].

I.2.5 Thin film growth mechanism:

All thin film processes are done in three stages:

- The production of appropriate ionic, molecular, atomic species.
- The transport of these species to the substrate.
- Condensation on this same substrate is done either directly or through a chemical or electrochemical reaction in order to form the solid deposit; this step often goes through three phases: nucleation, coalescence then growth.

.a) Nucleation

It is the phenomenon that accompanies changes in the state of matter and which consists in the appearance, within a given medium, of transformation points from which a new physical or chemical structure develops.

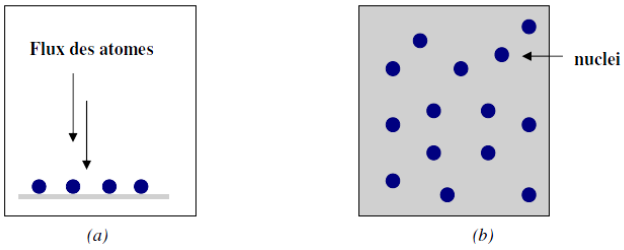

Figure I.3: Diagram of the nucleation of thin layers. a) The arrival of atoms on a substrate, b) The morphology of the substrate [10].

The entire surface of it, in this state, they interact with each other and form what are called "clusters". These "clusters" also called nuclei, are unstable and tend to subside. Under certain deposit conditions, they collide with other adsorbed species and start to grow. After reaching a critical size, these clusters become thermodynamically stable and the nucleation barrier is crossed. The nucleation stage is shown in figure I.3.

b) Coalescence

The nuclei grow in size but also in number until they reach a maximum nucleation density. This as well as the average size of these nucleus also called islets depend on a certain number of parameters such as the energy of the sprayed species, the rate of spraying, the energy of activation, adsorption, desorption, thermal diffusion, substrate temperature, topography and chemical nature of the substrates .

A nucleus can grow at the same time parallel to the substrate by a surface diffusion phenomenon of the pulverized species. It can also grow perpendicular to the substrate by adding sprayed species. In general the lateral growth in this stage is much more important than the perpendicular growth. Figure I.4 represents the phase of coalescence.

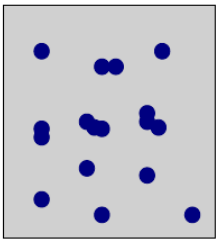

Figure I.4: Diagram representing coalescence [10].

c) Growth

The last step in the film manufacturing process is the coalescing step in which the islets begin to cluster. This tendency to form larger islets is improved by the growth of the surface mobility of the adsorbed species. This improvement is obtained by increasing the temperature of the substrate.

These larger islets still grow, leaving channels and holes on the substrate. The structure of the film in this step changes from a type of discontinuous islands to a type of porous networks .A continuous film is formed by filling the channels and the holes [10].

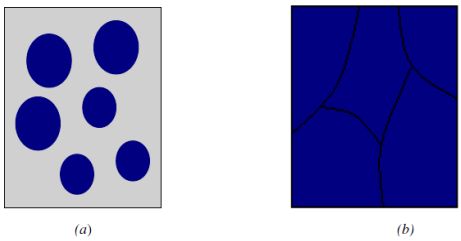

Figure I.5: The growth of thin layers. a) Step after coalescence, b) Growth [10].

I.2.6 Applications of thin films:

During the 20th century, more sophisticated applications diversified in the following fields **[11-12]**.

- ✓ **Microelectronics**: It was developed from the 1960s thanks to the use of increasingly thin conductive or insulating layers, and can be found under types of passivating layers (electronic contact), PN junction, transistor diode, piezoelectricity, laser, LED lamps, superconductors, etc.
- ✓ **Optics**: While retaining the aesthetic applications, the optical applications of the layers have made it possible to develop more effective radiation sensors, such as anti-reflective layers in solar cells, anti-reflective treatment of camera lenses, photo detection, display of screens dishes, ophthalmic applications, optical guides (architecture energy checks, vehicles, energy conversion, etc.).
- ✓ **Mechanics**: Tribological coatings (dry lubrication, resistance to wear, erosion, abrasion, diffusion barriers) micro-systems…etc.
- ✓ **Chemistry**: The main applications of surface coatings are oriented towards better corrosion resistance by the creation of a waterproof film (corrosion resistance), gas sensor, catalytic coatings and protective layers.
- ✓ **Thermal**: The use of a thermal barrier layer (TBC) decreases for example the surface temperature of the metal of the fins of the reactors thus making it possible to improve the performances of the reactors (increase in the internal temperature).
- ✓ **Biology**: Biological micro sensors, biochips, biocompatible materials…etc.
- ✓ **Micro and Nanotechnologies**: Mechanical and chemical sensors, micro fluidics, actuators, detectors, adaptive optics, nano-photonics…etc.
- ✓ **Magnetic**: Information storage (computer memory), security devices, sensors, etc.
- ✓ **Decoration**: Watches, glasses, jewelry, household equipment, etc [13].

I.2.7 NiO thin films:

Recently, NiO thin films were increased rapidly due to their importance in many applications in science and technology. NiO is one of the important p-type classes of semiconducting materials, which has attracted a good amount of research interest. This is because of the fact that NiO has unique optical, electrical and magnetic properties and founds

a vast diversity of applications in energy efficient smart windows, automobile mirrors, building glazing, optoelectronic devices and hetero-junction solar cells… etc[14].

Nickel Oxides is a wide band gap, low cost, advantageous ion storage material in points of cyclic stability and find applications in electro-chromic devices transition metals, which reversibly changes the optical properties in the presence of electric field. Furthermore, NiO was applied to produce the Ni-Cd rechargeable batteries. NiO is now exploited in the recyclable protein separation and as biosensors. In addition, there are many applications and properties of Nickel Oxide based materials were investigated and proved in the field of antimicrobial activity, control infections and excessive antibiotic resistance [15-16].

I.3 Fundamental properties of Nickel (Ni), Nickel Oxide (NiO) and Cobalt (CO) material

I.3.1 Nickel (Ni):

Nickel is a strong, lustrous, silvery-white metal that is a staple of our daily lives and can be found in everything from the batteries that power our television remotes to the stainless steel that is used to make our kitchen sinks (figure I.6).

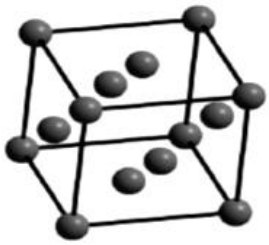

Figure I.6: Crystallographic structure of Nickel [17].

I.3.1.1 General Properties

- Atomic Symbol: Ni
- Atomic Number: 28
- Element Category: Transition metal
- Density: 8.908 g/cm^3
- Melting Point: 1455 °C
- Boiling Point: 2913 °C
- Moh’s Hardness: 4.0

I.3.1.2 Characteristics

Pure Nickel reacts with Oxygen and, therefore, is seldom found on the earth's surface, despite being the fifth most abundant element on (and in) our planet. In combination with Iron, Nickel is extremely stable, which explains both its occurrence in Iron-containing ores and its effective use in combination with Iron to make stainless Steel. Nickel is very strong and resistant to corrosion, making it excellent for strengthening metal alloys. It is also very ductile and malleable, properties that allow its many alloys to be shaped into wire, rods, tubes and sheets.

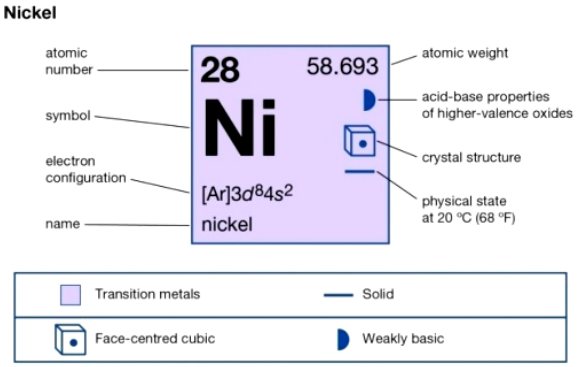

Figure I.7: Nickel metal profile [17].

I.3.1.3 Applications

Nickel is one of the most used metals on the planet. According to the Nickel Institute, the metal is used in over 300,000 different products. Most often it is found in Steels and metal alloys, but it is also used in the production of batteries and permanent magnets. [18].

I.3.2 Nickel oxide (NiO):

I.3.2.1 General properties

- Average atomic number : 18
- Average atomic mass (g) : 27.35
- Molar mass (g / mol) : 74.69
- Boiling point (° C) > 2000
- Solubility in water (mg / L) : 1.1 at 20 ° C. insoluble
- Melting point (° C) : 1990 - 1960
- Enthalpy of formation at : 298k -240 KJ / mole of atoms
- Entropy S_0 ($KJ.mol^{-1}$) : 38.0

I.3.2.2 Physical and chemical properties

Nickel Oxide (synonymous to Nickelous Oxide, green Nickel Oxide, Nickel monoxide) also known as bunsenite after R. Bunsen, was discovered in 1858 and is only found pure in nature in a few locations around the world. Nickel (II) Oxide has the chemical formula NiO and is a chemically stable material. NiO is the most main marketable forms of refined, relatively pure Nickel [19] .NiO actually very rare in nature, therefore, is typically produced artificially. Around numerous million of kilograms are formed annually [20] .NiO mainly exists in two forms such as black NiO and green NiO. The green crystal has almost exactly the stoichiometry composition of one Ni to one O atom, corresponding to the formula Ni1.00 O1.00.The black material has an excess of Oise, a deficiency of Ni with formula averaging Ni0.98 O1.00 and belongs to the class of non-stoichiometry compounds. NiO is negligibly soluble; solubility in water is 1.1 mg/L at 20 °C, the density of NiO is 6.67 $g.cm^{-3}$And the melting point is 2233 K. [19] .Numerous techniques used to produce NiO. Among this, heating greater than 400 °C, Nickel powder with the company of Oxygen this leads to the production of NiO. Also, green nickel oxide can be made using a heating mixture of Nickel powder compound and water at 1000 °C, this method was used in several commercial processes, the rate for this reaction can be increased by the addition of NiO [21-22].

I.3.2.3 Crystal structure

Nickel Oxide crystallizes in a rock salt type lattice as shown in figure I.8 each cubic unit cell has four Nickel atoms and four Oxygen atoms. Each Nickel atom is bounded by six Oxygen atoms and the same thing for Oxygen atom has six Nickel atoms surrounding it. This face-centered cubic (F.C.C) structure has a parameter of 4.1769Å at 26°C and the space group is Oh5 (Fm3m). Along any one of its triad axes, the (F.C.C) structure has a primitive rhombohedral cell with α = 60°. Figure I.8 shows a rhombohedral unit cell in the face-centered cubic cell. For nickel oxide, X-ray diffraction shows that the cubic lattice is slightly shifted to give a structure of rhombohedral cell with α =60°4.2' at room temperature. The Nickel-Nickel distance is 2.9518A for the distorted rhombohedral (α =60°4.2' at 18°C), while this distance should be 2.9535Å for a cubic cell (α =60°and a= 4.1769Å). This departure from the ideal-face centered cubic structure also was found to be temperature dependent. The amount of the distortion increases with the decrease of temperature [23-24].

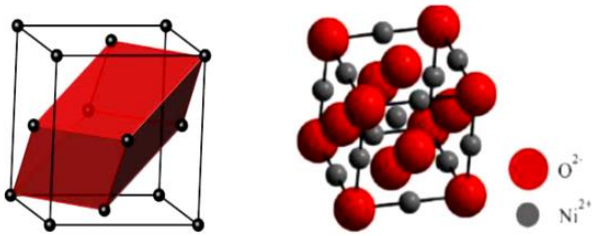

Figure I.8: The rhombohedral primitive cell of a face central cubic cell of Nickel Oxide [24].

Figure I.9 shows the phase diagram of a Ni-O binary system. The stable crystal structure of Nickel Oxide at a high temperature is polymorph bunsenite. By cooling the crystal, NiO converts to rhombohedral. It should be mentioned that these crystal structures form during thermodynamically stable transitions [24].

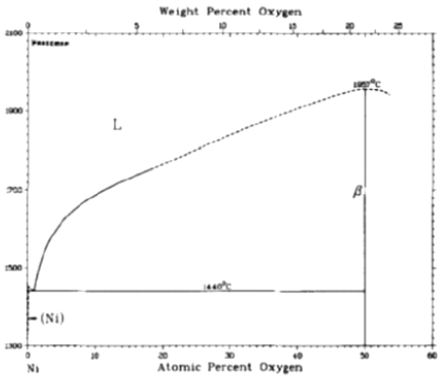

Figure I.9: NiO phase diagram [24].

I.3.2.4 Nickel thermal oxidation

Oxidation of the Nickel has been a subject of great interest during almost a century, due to its application in several technologies. Bunsenite (NiO), as explained before, is one of the most common phases of Nickel Oxides. Other phases such as Ni_2O_3 and NiO2 have also been claimed [25-26] .These investigations, as shown before, concluded that NiO is a metal with a p-type semiconductor, in which Nickel vacancies are the dominant defects. Some typical thermodynamic characteristics for Nickel and NiO are presented. It is also possible to plot the behavior of *G* in an Ellingham diagram figureI.9 for the reaction I.1.

$$2Ni + O_2 \longrightarrow 2NiO \qquad \text{(I.1)}$$

Table I.1: Standard thermodynamic properties of Nickel and Nickel Oxides [22].

	ΔH_f (kJ mol^{-1})	ΔG_f (kJ mol^{-1})	ΔS_f (kJ mol^{-1})
Ni(s)	0	/	29.9

NiO(s)	-239.701	-211.539	37.991

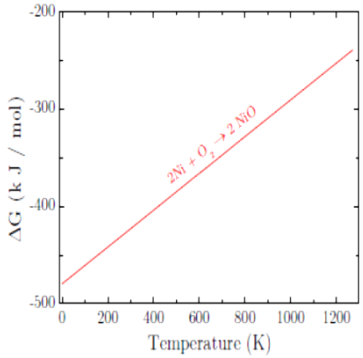

Figure I.10: Gibbs free energy versus temperature in Nickel Oxidation for the formation of NiO [27].

The conversion of Nickel that occurs in the oxidation route is predicted to follow thereactionI.1.Using the Gibbs free energy and the shown in table I.1, it is possible to achieve that the reaction I.1is favorable ($\Delta G < 0$) and the NiO structure is formed.

I.3.2.5 Defects and impurities in NiO crystal

Crystalline solids show a periodic of atom in the crystal structure. A perfect stoichiometry metal oxide is an insulator and by introducing different defects inside the crystal, the mechanical, optical and electrical property of the oxide changes, respectively.

Various categories of defects inside the crystal can exist such as point, line, planar and bulk defects. Point defects are common in different crystals due to a small size of impurity atoms in the material. Interstitial, substitution atoms and vacancies are common examples of point defects in the crystal. FigureI.11 shows different point defects in a crystal. Dislocations (edge, screw or mixed) are examples of line defects. Planar defects can be devised into grain boundaries and stacking faults. The grain boundaries occur when various crystallographic planes reach together. The stacking fault structure is common in closed packed structures such as FCC and HCP and is caused by misalignment of several layers of atoms in a preferred orientation. The physical properties of a sample may be altered by modifying the defects number in the crystal. Fabrication processes, the percentage of impurities and annealing temperature have strong parameters affected by the film properties [28].

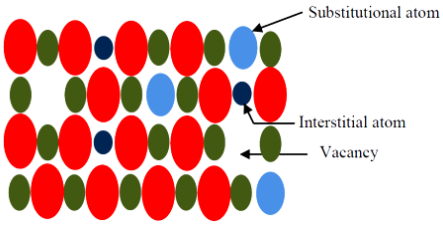

Figure I.11: Type of defects inside crystal [28].

I.3.2.6 Optical properties

Nickel Oxide is a bread band-gap semiconductor. The absorption edge is localized in the ultraviolet region, the existence of Ni^{+3}ions inner the oxide lattice shows charge transfer transition with the resulting absorption in the visible region [29-30].Various researchers have estimated the absorption of photon energy for NiO [31-32].Reported gap energy value for the NiO is in the range of 3.6 to 4 eV, however, the refractive index is 2.33 at the photon energy of 2 eV [33].The valence band consists of localized Nickel 3d-bands with a width of 4.3-4.4 eV [34-35] .at about 2eV above the Fermi level at –8.74 eV. Oxygen at the 2p band with large energy about 4–8 eV; were coupled with the Nickel 3dstates. However, the conduction band composes of unoccupied states of Nickel 3d, 4s, and 4p [36]. Two main theories proposed for explaining the optical absorption gap in NiO: it is due to either a p⟶d transition in one Ni atom [37].or a d⟶ d transition throughout two adjacent Ni atoms in the lattice [38].

I.3.2.7 Electrical properties

NiO has p-type oxide semiconductor character with broadband gap energy. Nominally pure stoichiometry NiO is an insulator as in figure I.13 with a room temperature resistivity of the order of $10^{13}\Omega$-cm is classified as a Mott-Hubbard insulator. Various theories have been done to explicate the insulating behavior of NiO; they include localized electron theory, band theory, chemical band approach and cluster theory. After intense theoretical and experimental investigations, the electronic structure of NiO remains controversial [39].

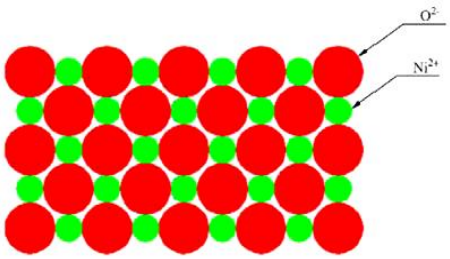

Figure I.12: A schematic of pure stoichiometry NiO crystal [28].

Stoichiometry NiO is pale green. Black color in NiO has been attached to the appearance of Ni^{+3}ions. Such ions are present in NiO as charge compensation for Nickel

vacancies [40]. Different samples have different conductivities suggesting conduction is dominated by the effect of random impurities or lattice defects. The appearance of Nickel vacancies besides some other impurities like OH^-, CO_3^{2-} in defect nickel oxide affects the electronic structure of the Oxygen atom where extra O1s peaks with greater binding energy are observed by XPS also the typical O1s peaks of Oxygen in stoichiometry NiO [41] .Electronic conduction in non doped NiO is suggested to the appearance of Nickel vacancies or excess of Oxygen. In the ionic crystal of NiO, the orientation of the film is usually affected by the orientation of O^{-2} when the active species of Nickel and Oxygen impinge separately on the growth of the film surface. This is because NiO has no directivity of a mixture between Ni^{+2} and O^{-2} and the radius of O^{-2}(0.140 nm) is superior to that of Ni^{+2}(0.069 nm) [42] .The Oxygen atom is too large to permit any considerable concentration of interstitial O atoms in the structure. As a resulting overload of O in NiO create vacancies in the normally occupied Ni sites as in figureI.14. However, to preserve overall electrical neutrality in the crystal, two Ni^{+2}ions should be converted to $Ni^{+3}$for every vacant Ni^{+2}sites. The Ni^{+3}ions introduced within the crystal in this way can be advised to be positive centers capable of jumping from one Ni^{+2} site to another. When an electron hops from a Ni^{+2} to a Ni^{+3}sites, it is as if a positive hole moves around the Ni^{+2}sites. Thus overload of Oxygen makes the NiO as p-type semiconductor [22].

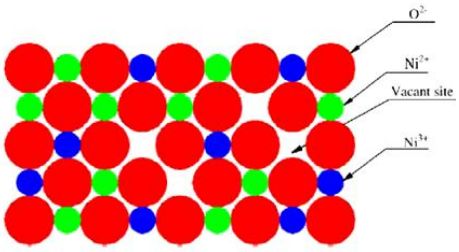

Figure I.13: A schematic of pure non-stoichiometry NiO crystal [22].

I.3.2.8 Magnetic properties

Any modification in the structure of crystal with temperature actually is interrelated with the magnetic properties of NiO. The Néel temperature (T_N) is the temperature at which ant ferromagnetism changes to par magnetism. Nickel oxide is ant ferromagnetic at room temperature and paramagnetic above its Néel temperature T_N=250°C. At a temperature above T_N, the structure of the crystal is cubic; whereas below T_N, the lattice structure becomes distorted to rhombohedral. This distortion consists of diminution in the cubic structure along the (111) axes. Furthermore, the spin configuration in nickel oxide has been validated using neutron diffraction work. FigureI.15 shows the ordered arrangement of spin of the Nickel

ions in NiO under the T_N temperature. Apparently; each magnetic unit cell contains four chemical unit cells [43].

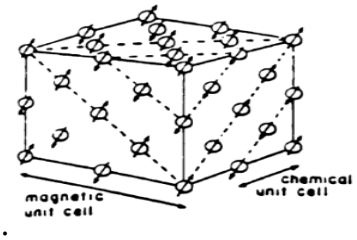

Figure I.14: Ordered arrangement of spins Ni^{+2} ions in NiO/the O^{-}ions are not shown [43].

I.3.2.9 Applications

Nickel Oxide thin films have been employed as:

- ✓ An ant ferromagnetic material.
- ✓ P-type transparent conducting films.
- ✓ Electro catalysis.
- ✓ Positive electrode in batteries.
- ✓ Fuel cell.
- ✓ A material for electro-chromic display devices.
- ✓ Part of functional sensor layers in chemical sensors.
- ✓ Solar thermal absorber.
- ✓ Photo electrolysis.
- ✓ Promising ion storage material in terms of cyclic stability.
- ✓ Resistive memories.
- ✓ Electro-chromic devices.
- ✓ Giant magneto resistive spin valve structures.

I.3.3 Some properties of cobalt:

Cobalt is a naturally occurring element in the environment: water, earth and rocks. It does have certain benefits for humans; however, at too high concentrations it can be harmful [45].Cobalt is a chemical element, transition metal, symbol CO, number atomic 27 and molar mass 59 g / mol. Cobalt has two common oxides: COO and CO_3 O_4In aqueous solution, the stable form of Cobalt is the CO^{+2} ion [46].

I.3.3.1 General properties

- ρ (g.cm − 3) at: 20 ° C 8.83

- Tfusion (° C) at: 1459
- Tevap (° C) at: 10−4 Tor 1530
- Structure: CFC
- a (Å): 3.55
- Chemical formula: CO

I.4 Deposition methods

I.4.1 Criteria for selection of deposition methods:

The selection of a specific technology for the deposition of thin films can be based on a variety of considerations. A multitude of thin films of different materials can be deposited for a large variety of applications; hence, no general guidelines can be given of what the most suitable deposition technology should be. In selecting an appropriate deposition technology for a specific application, several criteria have to be considered.

In order to optimize the desired film characteristics, a good comprehension of the advantages and restrictions applicable to each technique is necessary. The choice of a specific deposition technique related to some factors, they are:

- The material to be deposited.
- The rate of deposition.
- Limitations imposed by the substrate, e.g.: maximum deposition temperature.
- Adhesion of the deposits to a substrate.
- Throwing power.
- The purity of target material.
- Availability of the required equipment.
- Cost.
- Ecological considerations.
- The abundance of the material (to be deposited).

I.4.2 Different deposition techniques:

The properties and versatility of the thin films can be obtained by selecting proper technique of film deposition. Thin film deposition methods can be broadly classified as either chemical or physical methods. The difference between the chemical and physical thin film deposition methods depends upon the method of depositing thin film material on the substrate. In chemical deposition technique, fluid precursor is used which chemically react

with the substrate. Since the thin film material is conducted through the fluid precursor, physical deposition is conformal approaching the substrate without preference to a particular direction. A conformal is an uneven interface with the body and has a constant thickness on horizontal and vertical surfaces [47].

The broad classification of deposition techniques is outlined in the figureI.17. An enormous number of deposition processes that exist and just only some methods are detailed in the next parts with special emphasis on our processes “the spray pyrolysis method” [48].

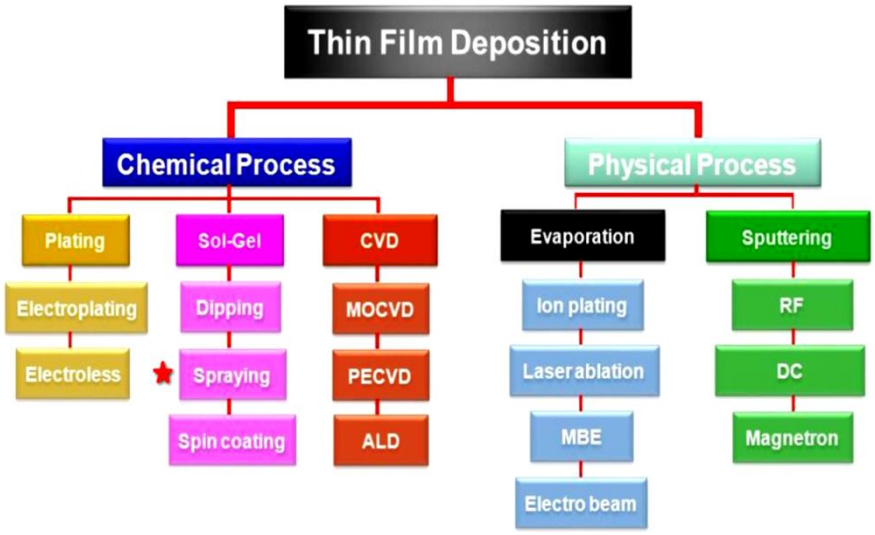

Figure I.15: Schematic diagram of classifications of thin films deposition techniques [48].

I.4.2.1. Physical methods of deposition

Physical deposition uses thermodynamic or mechanical means to fabricate required thin films. These techniques are costly but offer relatively more reliable and further reproducible results. Furthermore, the physical methods need high energies, and chemical reactions are not used to store these energies .Commercial physical deposition systems favor requiring a low-pressure vapor medium to function properly [49].

I.4.2.1.1 Evaporation under vacuum

The vapor of the material to be deposited is obtained by heating it, by different processes: the resistance or Joule effect oven; induction; electronic bombardment figure I.18 and laser beam. In evaporation, the deposition rate depends essentially on the vapor pressure of the material to evaporate, that's why the deposition process takes place under a secondary vacuum (generally 10^{-3} and 10^{-5} mBar) [50].

As the vapor flow is localized and directional, it is necessary to print on the substrate a movement of rotation or translation relative to the source of evaporation, so as to achieve uniform deposits and uniform thickness. The best results are obtained on surfaces practically perpendicular to the flow of vapor. When the pressure is not low enough the deposits are poorly adhesion and often amorphous [51].

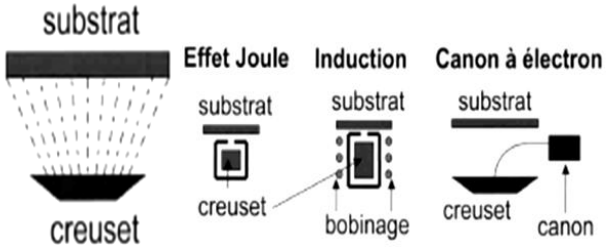

(a) (b)

Figure I.16: (a) Schematic diagram of evaporation, (b) Heating processes using vacuum evaporation [51].

I.4.2.1.2 Cathode sputtering

Sputtering is one of the oldest techniques. Heavy ions of a rare gas, generally Ar^+, are accelerated under high voltage to the cathode which is made up of the target material to be deposited. The surface atoms will then be torn off and projected towards the cooled substrate in order to deposit there. The ionization of the Argon atoms is carried out in a vacuum chamber reaching 10^{-6} Torr. An electric discharge occurs in the enclosure after applying a voltage between two planar electrodes: a cathode where the target of the material to be deposited is installed and an anode which is generally connected to the ground which carries the substrate to be covered. The Argon ions (Ar^+) created in the discharge are accelerated towards the cathode and thus acquire the energy which they release during their impact on the surface of the target. This can lead to the ejection of atoms which deposit on the substrate. A schematic diagram of the operation of sputtering is presented in figure II.19. The physical mechanisms of spraying are dealt with in numerous works.

Spraying techniques are generally used to deposit all kinds of materials: metals, refractory materials, dielectrics, and ceramics. The main difficulty of spraying is to control the final composition of the layer. In fact, the energy of the incident Argon ions is greater than the binding energy of the target atoms, which means that the particles expelled, are in atomic form and the sputtering rates vary from one compound to another. The stoichiometry of the target is therefore not respected. Although this problem of difference between the

compositions of the primary material and of the final layer also exists in sol gel and in MOCVD, it is more difficult in spraying to redo a new target for each new test.

Despite these difficulties, spraying remains the cleanest technique and ensuring good homogeneity of the layer and strong adhesion to the substrate [52].

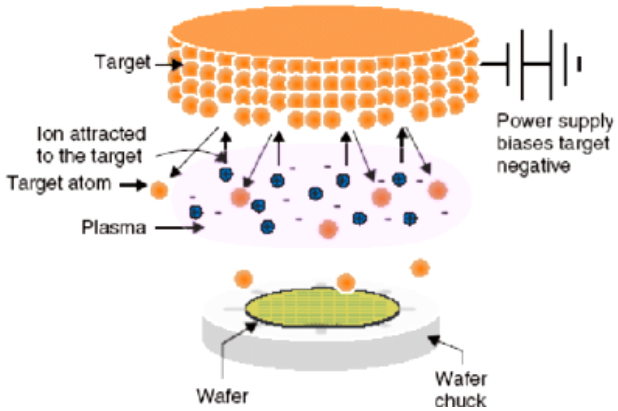

Figure I.17: Cathodic sputtering: accelerated Ar + ions extract atoms from the target [53].

I.4.2.1.3 Pulsed laser deposition

It is an ablation process. High power pulses of laser light are focused on the surface of the target material in a vacuum chamber [54-55] .This results in vaporization of the target material. The atoms ablated from the target material get deposited on the substrate. Figure I.20 shows pulsed laser deposition technique.

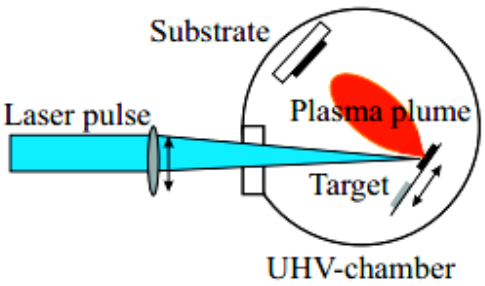

Figure I.18: Pulsed laser deposition technique [54].

I.4.2.1.4. Thermal evaporation

The thermal evaporation process contains evaporating source materials in a vacuum chamber below 10^{-6} Torr and condensing the evaporated particles on a substrate. In this process, thermal energy is provided to a source from which atoms are evaporated for deposition in the substrate. Heating of the source material can be finished by any of which the

material to be evaporated is attached. Larger volumes of source material can be heated in crucibles of refractory metals, Oxides or Carbon by resistance heating, high-frequency induction heating, or electron beam evaporation. The evaporated atoms travel through reduced background pressure in the evaporation chamber and condense on the growth surface. The deposition rate or flux is a function of the travel distance from the source to the substrate, the angle of impingement onto the substrate surface, the substrate temperature Ts, and the base pressure. The conventional thermal evaporation system is mentioned in figureI.21 [56-57].

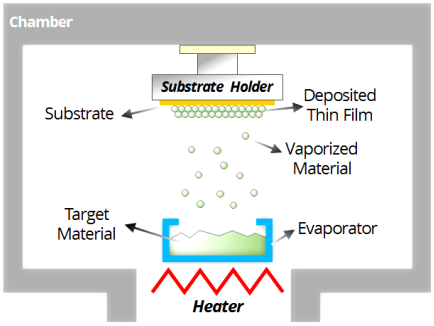

Figure I.19: Schematic diagram of thermal evaporation system [58].

I.4.2.2 Chemical method of deposition:

Chemical deposition processes are the most significant techniques for the growth of films owing to their versatility for depositing a very large number of elements and compounds at relatively low temperatures. The processes are very economical and have been industrially exploited to a large scale [49].

I.4.2.2.1 Chemical bath deposition

The chemical bath deposition (CBD) is also recognized as controlled precipitation; it has been applied since to deposit films of many different semiconductors. It is currently attracting great attention as it does not necessitate sophisticated instrumentation like vacuum system and other expensive equipment. All that is required is a vessel to include the solution (an aqueous solution made up of a few usually common, chemicals) and a substrate on which deposition is required. It offers a bottom-up approach to prepare nano-crystalline materials in thin film form with better particle size controlled, particle shape, size distribution, particle composition, the degree of particle agglomeration, the conventional thermal evaporation system is presented in figureI.22 [59].

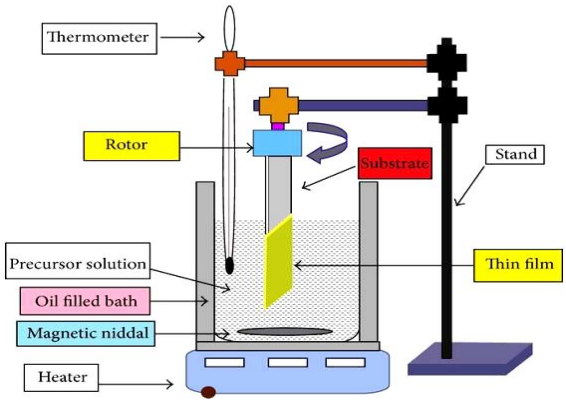

Figure I.20: Schematic diagram of chemical bath deposition system [59].

I.4.2.2.2 Electro-deposition

The appearance of chemical changes due to the transition of electric current via an electrolyte is named electrolysis and the deposition of any substance on an electrode as a consequence of electrolysis is called electro deposition as mentioned in figureI.23. This phenomenon is dominated by the two following laws, first enunciated by Faraday in 1833: (i) the magnitude of chemical change occurring is relative to the electric current passed and (ii) the masses of different kinds deposited at or dissolved from electrodes in the similar quantity of electricity are in direct proportion to equivalent weights. The two laws can be united and expressed mathematically as:

$$W = \frac{IEt}{F} \qquad (I.2)$$

Where:

W**:** is the mass (in g) of the deposited material, I is the current (in A), E is the chemical equivalent weight (in g), and t is the reaction time (in s). F constant called the Faraday, equivalent to 96500 C and is defined as the quantity of charge necessary to deposit one equivalent of any ion from a solution [60].

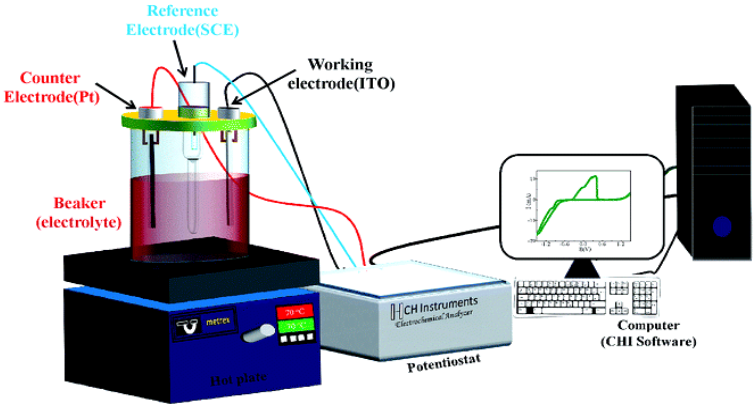

Figure I.21: Schematic diagram of electro-deposition system [61].

I.4.2.2.3 Chemical vapor deposition

Chemical vapor deposition (CVD) is the condensation of chemical compounds from the gas phase onto a substrate where the reaction occurs to produce a solid deposit. The gaseous compound, bearing the deposited material, if not already the vapor state is formed by volatilization from either a liquid or a solid feed and is caused either to flow by a differential of pressure or by the achievement of gas transported into the substrate. The chemical reaction is started approximately to the surface of the substrate which produces the desired material. In some processes, the chemical reaction may be activated through an external agency such as an application of heat, RF field, light or X-rays, an electric arc or glow discharge, electron bombardment etc. The microstructure, morphology and adhesion of the deposit are greatly related to the activation process and the nature of the chemical reaction [62].

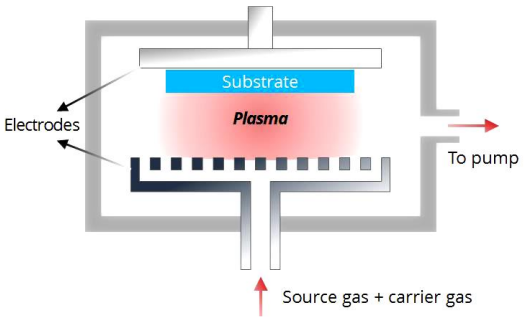

Figure I.22 : Plasma chemical vapor deposition [63].

I.4.2.2.4 Sol-gel technique

The sol-gel process is one of the mainly useful solution deposition methods of thin films. 'Sol' includes metal salts or metal “alkoxides” as precursors (starting material) and their appropriate solvents. Moreover, the sol may contain some functional additives like stabilizers that chemically improve the sol homogeneity. The liquid-filled solid network called “gel” is originated by the linking of colloidal particles with one another in 3D structure.

The transformation from sol to gel is most commonly provoked by changing the PH value of the sol via catalysts such as acids and bases. The catalysts initiate the sol to gel transformation by affecting the overall hydrolysis and condensation rates.

As a result, characteristic of gel, such as the structure of the chains or groups, appropriate time for gelatin. Sol-gel offers a low-temperature route for the production of complex/functional oxide structures and deposition of sol onto complex-shaped or large surfaces. It has several chemical and physical steps which are hydrolysis, condensation, drying, and densification. It is possible to fabricate high purity products such as micro and nano-particles in different size/shape, fibers, membranes, powders and coatings by a sol-gel process. The schematic

summary of this technique is given in figureI.25. This technique is promising with its low cost, simple equipment requirement and scalability [64].

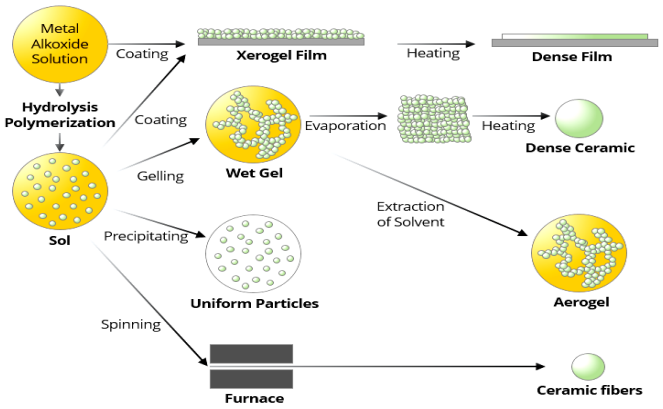

Figure I.23: Schematic summary of the sol-gel process [64].

I.4.2.2.5 Spray pyrolysis technique (SPT)

A) Introduction

In 1966, Chamberlin and Skarman for the first time used spray pyrolysis technique (SPT) for the preparation of CdS thin layers and application in a solar cell. SPT is a process to elaborate dense and porous oxide films, ceramic coatings, and powders. Compared with other film deposition techniques, SPT represents a very simple and relatively cost-effective method, especially regarding equipment cost. SPT does not necessitate high-quality substrates or chemicals. This method has been used for the deposition of dense films, porous films, and for powder production. Even multilayer films can easily be elaborated using this versatile technique. SPT has been used for several decades in the glass industry and in solar cell production to deposit electrically conducting electrodes [65].

B) The principle

The deposition of film from the spray pyrolysis method requires heated substrate in order to spray the metal salt from the aqueous solution. Droplets were scattered and formed disk-shaped structure into the surface of the substrate and undergo thermal decomposition.

The size and shape of the disk correlated with substrate temperature, the volume, and momentum of the droplet. Consequently, this film was produced and included overlapping disks of metal salt being changed to metal oxide. Some types of spray pyrolysis devices are developed to exploit the capability of the technique coupled with the properties of the solution

precursors. The change in atomization method resulted in different spray pyrolysis techniques. They are [66]:

- Pressurized air blast (liquid is exposed to a stream of air).
- Ultrasonic wavelengths were produced and are required for fine atomization.
- Electrostatic (liquid interacts with the existence of high electric field).

Out of all these, pressurized air blast spray deposition is the most simple and cost-effective. The spray parameters can be very well controlled. The fundamental of spray pyrolysis components is spray nozzle, a rotor for a spray nozzle, liquid level monitor, hot plate, gas regulator valve and air compressor as it mentioned in figureI.27.

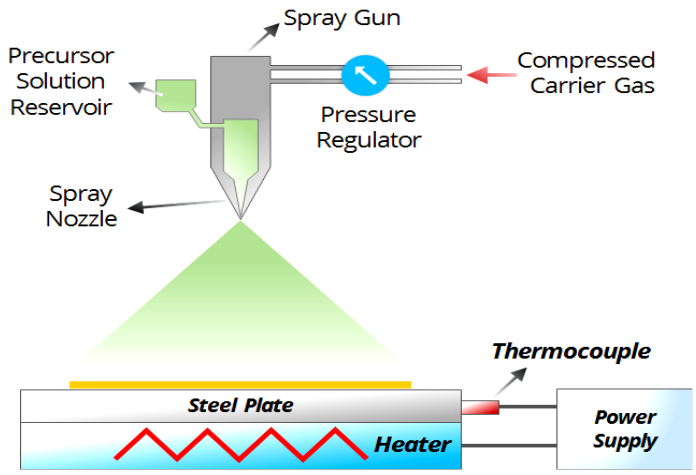

Figure I.24: Schematic diagram of spray pyrolysis system [67].

C) Scheme of pyrolysis and formation of thin films:

In spray pyrolysis, the experimental parameters such as precursor solution, decomposition of the precursor, atomization, and aerosol transport are very significant in order to examine the structural, compositional, surface topology, electrical and optical properties of the thin films. Several of these parameters are investigated in the following section.

a/ Precursor solution

Precursor solution shows as the main important parameter in the production of thin films from different compounds. Aqueous solutions are typically used due to low cost, the simplicity of handling and existence in the wide range of water-soluble metal salts. The solute must have high solubility, for maximum yield. Alcoholic and organic solutions have been applied to synthesize the organic materials of non-oxide ceramic solutions.

b/ Atomization of precursor solution

The critical operation of the spray pyrolysis method is to produce homogeneous surface and silky droplets by thermal decomposition. A different atomization methods such as; pneumatic, ultrasonic and electrostatic have been applied for solution aerosol formation. Some of spray atomization methods like electrostatic spray pyrolysis, microprocessor-based spray pyrolysis, radiance spray pyrolysis, ultrasonic nebulizer atomization technique etc are also being used. These previous atomizers types vary in velocity of a droplet, size of droplet and rate of atomization. The size of the droplets was produced with pneumatic or pressure nozzles decrease when a difference of the pressure across the nuclei is increased.

c/ Decomposition of precursor

When a droplet strikes on the surface of the substrate the processes like evaporation of the residual solvent, spreading of the droplets and salt decomposition takes place. Many models exist for demonstrating the decomposition of a precursor. Various steps during pyrolysis of aerosols are as explained below figure I.28 [68].

- In the primary step, an aqueous precursor solution is converted into aerosols (droplets) by spray nozzle and the solvent evaporation takes place.
- In this step, the solvent is vaporized which induce the formation of precipitate as the droplets approach the substrate.
- When the precipitate arrives at the substrate, nucleation and the growth of thin films on the substrate take place.
- The final step, the growth of the nuclei which accompanied to the production of the continuous thin film layer.

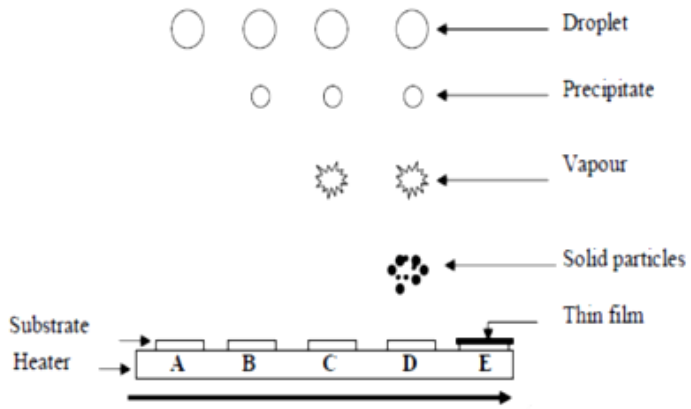

Figure I.25: Mechanism of thin films formation by spray pyrolysis method [69].

D) Advantages of chemical spray pyrolysis technique:

Chemical spray pyrolysis technique has a number of advantages as depicted in the following points [70-71]:

1. It offers an extremely easy way to dope films with virtually any element in any proportion by merely adding it in some form to the spray solution.
2. Unlike closed vapor deposition method, SPT does not require high quality targets and/or substrates, and it does not require vacuum at any stage, which is a great advantage if the technique is to be scaled up for industrial applications.
3. The deposition rate and the thickness of the film can be easily controlled over a wide range by changing the spray parameters, thus eliminating the major drawbacks of chemical methods such as sol-gel method which produces films of limited thickness.
4. Operating at moderate temperatures (100 – 500 ºC), SPT method can produce films on less Robust materials.
5. Unlike high – power methods such as radio frequency magnetron sputtering (RFMS), it does not cause local over – heating that can be detrimental for materials to be deposited.
6. By changing composition of the spray solution during the spray process, it can be used to Make layered film and films having composition gradients throughout the thickness.
7. It is believed that reliable fundamental kinetic data are more likely to be obtained on particularly well characterized film surface, provided the film are quiet compact, uniform and that no side effects from the substrate occur, SPT offers such an opportunity.
8. Low cost comparing with other methods which require complex devices and instruments with high cost.

I.5 Conclusion

Through this chapter, we defined the thin film. Then we presented general properties of Nickel, Nickel Oxide followed by Cobalt. At the end of the chapter we explained some preparation methods of films and we focused on the method of spray pyrolysis and their advantages.


Chapter 2

II.1 Introduction

This chapter includes two parts A and B, the first part we pay particular attention to the different steps of our experimental work in a detailed way. While in the second part, we present the characterization techniques used in our work to measure the different properties (structural, optical and electrical).

II.2 Part A: Experimental Work

II.2. 1 Experimental condition:

- ✓ The Substrate temperature: 450 °C.
- ✓ Spout-Substrate distance: 24 cm.
- ✓ The Quantity of the solution: 5 ml.
- ✓ The Deposit time: 20 - 25 min.
- ✓ Pressure: 2 bar.

II.2. 2 Experimental setups:

❖ **Calculate weights:**

The weights were measured by sensitive electronic balance with four digits (10^4g) sensitivity figure II.1 .The appropriate weight of the materials $Ni(NO_3)_2.6H_2O$and $COCl_2.6H_2O$ were determined by using the following equation:

$$\mathbf{m = M \times C \times V} \qquad \text{(II.1)}$$

m: Mass Molar of the Powder (g).

M: Molar mass (mol).

C: The concentration (mol/L).

V: The volume of distilled water (L).

- ✓ **Calculate weight of $Ni(NO_3)_2.6H_2O$:**
  - $M_{Ni(NO3)2.6H2O}$= 290.81 g/mol
  - m_{Ni}= 58.693 g/mol

  m = M × C × V = 290.81×0.1×0.05

  $m_{Ni\ (NO3)2.6H2O}$ = 1.454 g

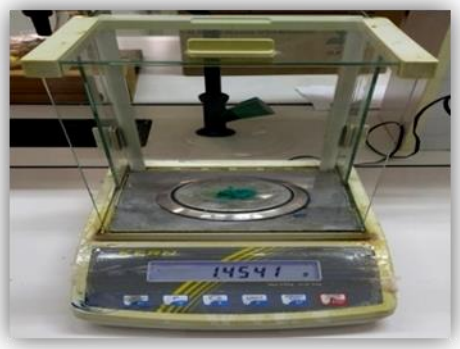

Figure II.1: Sensitive electronic balance with four digits (10^4g) sensitivity.

✓ **Calculate weight of Ni:**

$$m_{Ni} = \frac{m_{Ni(NO_3)_2.6H_2O} \times M_{Ni}}{M_{Ni(NO_3)_2.6H_2O}}$$

$$m_{Ni} = \frac{1.454 \times 58.693}{290.81}$$

$$m_{Ni} = 0.2934 \text{ g}$$

✓ **Cobalt Chloride doped:**

- $M_{COCl2.6H2O} = 237.928$ g/mol
- $m_{CO} = 58.933$ g/mol

$m_{CO} = m_{Ni} \times 1\%$ doped $= 0.2934 \times 0$

$m_{CO} = 0.002934$ g

✓ **Cobalt Chloride doped for 1%:**

$$m_{COCl2.6H2O} = \frac{m_{CO} \times M_{COCl_2.6H_2O}}{M_{CO}}$$

$$m_{COCl2.6H2O} = \frac{0.002934 \times 237.928}{58.933}$$

$$m_{COCl2.6H2O} = 0.012 \text{ g}$$

✓ **Chloride doped for 1.5 %:**

$m_{COCl2.6H2O} \times 1.5 = 0.012 \times 1.5 = 0.018$ g

✓ **Calculate weight of $COCl_2.6H_2O$:**

The different weight mass of the different percentage (0, 1.5, 3, 4.5, 6 and 7.5) % are calculated and presented in the table II.1.

Table II.1: The weights of powder used in the preparation of the solution.

Doped percentage (%)	Weights (g)
Non doped	$m_{Ni\ (NO3)2.6H2O} = 1.454$
1.5	$m_{COCl2.6H2O} = 0.018$
3	$m_{COCl2.6H2O} = 0.036$
4.5	$m_{COCl2.6H2O} = 0.054$
6	$m_{COCl2.6H2O} = 0.072$
7.5	$m_{COCl2.6H2O} = 0.09$

II.2. 3 Preparation of solution:

- **$Ni(NO_3)_2.6H_2O$:** Green powder of Nickel Nitrate is the primary source of materials, with 1.4541 g dissolved in 50 ml of distilled water at 50 °C with concentration of 0.1 (mol/L).

Product Specification

NICKEL (II) NITRATE (HEXAHYDRATE) AR

PRODUCT CODE	593745
SYNONYMS	[Nickel (II) nitrate hexahydrate]
C.I. NO.	--
CASR NO.	(13478-00-7)
ATOMIC OR MOLECULAR FORMULA	$Ni(NO_3)_2.6H_2O$
ATOMIC OR MOLECULAR WEIGHT	290.79
PROPERTIES	Melting point 55°C

$Ni(NO_3)_2.6H_2O$

PARAMETER	LIMIT
Description	Green crystals/crystalline powder.
Solubility	10% solution in water is bright and clear.
Minimum Assay (complexometric)	99.0%

Figure II.2: Profile of Ni $(NO_3)_2.6H_2O$ [72].

Figure II.3: Powder of Nickel Nitrate.

- **$COCl_2.6H_2O$:**

The solution was prepared by dissolving 1.454 g of Nickel Nitrate with the right weights of cobalt chloride. The appropriate different percentage (0.018, 0.036, 0.054, 0.072 and 0.09) g in 50 ml of distilled water at 50 °C with concentration of 0.1 (mol/L).

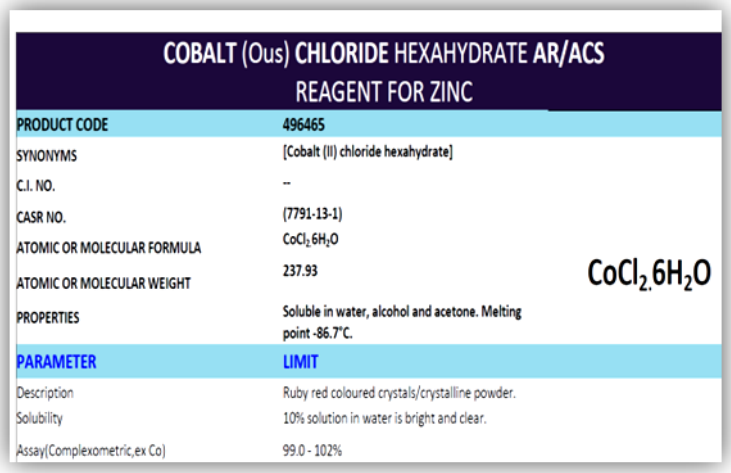

COBALT (Ous) CHLORIDE HEXAHYDRATE AR/ACS REAGENT FOR ZINC	
PRODUCT CODE	496465
SYNONYMS	[Cobalt (II) chloride hexahydrate]
C.I. NO.	--
CASR NO.	(7791-13-1)
ATOMIC OR MOLECULAR FORMULA	$CoCl_2.6H_2O$
ATOMIC OR MOLECULAR WEIGHT	237.93
PROPERTIES	Soluble in water, alcohol and acetone. Melting point -86.7°C.
PARAMETER	LIMIT
Description	Ruby red coloured crystals/crystalline powder.
Solubility	10% solution in water is bright and clear.
Assay(Complexometric,ex Co)	99.0 - 102%

$CoCl_2.6H_2O$

Figure II.4: Profile of $COCl_2.6H_2O$ [72].

Figure II.5: Powder of cobalt chloride.

❖The solution preparation steps are as follows:

- ✓ Added to 50 ml of distilled water, the necessary amount of Nickel Nitrate as well as the cobalt Chloride**.**
- ✓ Mixing everything with average speed of rotation using (Magnetic Stirrer) tray heated at temperature of 50 °C in 60 minutes to make sure that no residues were left and to ensure the homogeneity of the resultant solution figure II.6**.**
- ✓ The resultant solution put it in glass bottle and kept to cool at the temperature of the room for 24 h figure II.7**.**

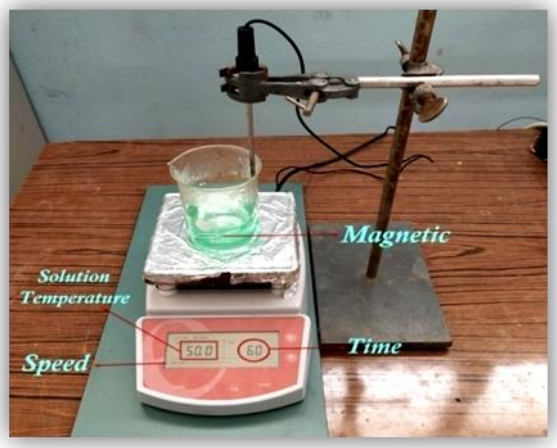

Figure II.6: (Magnetic stirrer) tray heated.

Figure II.7: Chemical Solution prepared.

This method of forming thin layers on glass substrates is done by the union.

The Nickel ions with the Oxygen ions present in the air of the furnace « case of non-doping».

$$2\,(Ni\,(NO_3)_2.6H_2O) \xrightarrow[450\ °C]{} 2Ni\downarrow + 4NO_2\uparrow + O_2\uparrow + 12(H2O)\uparrow \qquad \text{(II.2)}$$

The Nickel ions and those of Cobalt are associated with Oxygen ions at a temperature of 450 °C. This solution is prepared with different percentages of Co, as indicated in table II.2.

Table II.2: The volumetric ratios of the solutions used in the preparation of thin films.

doping (%)	**Solution of $Ni\,(NO_3)_2.6H_2O$**	**Solution of $COCl_2.6H_2O$**
Non doped	100	0
1.5	98.5	1.5
3	97	3
4.5	95.5	4.5
6	94	6
7.5	92.5	7.5

II.2. 4 Preparation of substrates:

A/Choice of substrate

This choice allows us to carry out a good optical and electrical characterization of the layers; we used glass microscope slides with the dimensions of (25.4 x 76.2 mm^2) and a thickness of 1-1.2 mm figureII.8.

The substrates used are glass slides; this choice of glass is due to three reasons:

1- It makes it possible to carry out a good optical characterization of the films which adapts well for their transparency.

2- After deposition, the sample (substrate + layer) will undergo a cooling from the deposition temperature above 450°C to ambient temperature (~ 25 °C) which causes compressibility of the two materials constituting the sample. In this case, they have very close expansion coefficients, which minimize the stresses. Note that an increase in the temperature of the substrate leads to an increase in stresses. This is linked to the compressive stress caused by the difference between the expansion coefficients of the substrate and of the material deposited :
(α glass = 8.5×10^{-6} K^{-1}, α NiO = 7.93×10^{-6} K^{-1}).

3- Economic reasons [73].

Figure II.8: Type of glass substrates used.

B/Cleaning of substrates

The cleaning of the substrate is very important because it has a great effect on the properties of the films and the step determines the qualities of adhesion and homogeneity of the deposited layers, The quality of the deposit and consequently that of the sample depends on the cleanliness and the state of the substrate, remove all traces of grease and dust and visually check that the substrate surface is free of scratches and flatness clear as crystal. These conditions are essential for the good adhesion of the deposit to the substrate, and for its uniformity (constant thickness).to do this, it is essential to go through the substrate cleaning process because the electrical characteristics are very sensitive to surface preparation techniques.

- The process can be summarized by the following steps:
  - Cleaning with (20 ml HCL + 100 ml distilled water) for 5 min at room temperature:

« To remove any traces of grease and impurities attached to the surface of the substrate».

  - Washing in a bi-distilled water bath for 5 min.
  - Cleaning with (5 ml Methanol + 5 ml Acetone) for 5 min:

«This reacts with contamination such as grease and some oxides».

  - Washing in a bi-distilled water bath.
  - And finally, drying using an electrical oven and Josef paper.
- Avoid touching the surface of the substrate to avoid contamination.

C/Cuts & remarks of substrates

The figure II.9 show the methods of cuts and remarks of the substrates to 3 section of (2.5× 2.5) Cm².

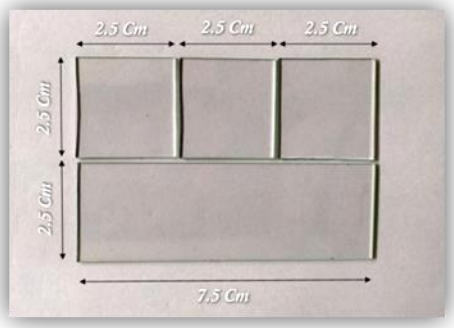

Figure II.9: The substrates cuts method.

II.2.5. System of chemical spray pyrolysis:

- Figure II.10-11show the chemical spray pyrolysis system used in the preset work.

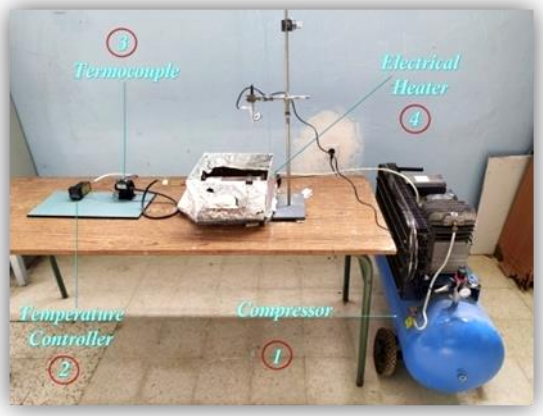

Figure II.10: Experimental setups of the pyrolysis spray system.

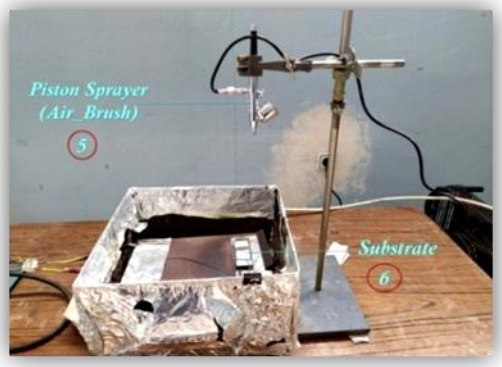

Figure II.11: Experimental device of the pyrolysis spray technique used.

❖ The main elements of this assembly are:

1. Air Compressor

Under a controllable pressure (P = 2 bar) the compressor pushes the pressurized air drop from glass bottle; this leads to make the solution flows from the capillary tube to the glass substrates, as soft spray.

2. Thermocouple

This includes a sensitive thermal wire; it is attached to the hot plate and joined to the digital temperature controller which fixes the temperature of the surface of the plate to the desired value.

4. Electrical Heater

The heater is used for heating the plate on which the glass substrate is placed, to deposit the thin film. In this study the temperature used was 450 ±30 ° C.

5. Airbrush

Figure II.12: Royal_Max airbrush gun [74].

II.2.6 Parameters affects the films deposition:

a) Air Pressure

In this study the air pressure was kept at (2 bar) to get uniform films the air pressure inside nozzle was adjusted to obtain fine atomizes in order to avoid the rapid decrease in substrate temperature which will cause the glass substrate to be broken.

b) Substrate Temperature

One of the important parameters is substrate temperature it significant affect the homogeneity of the prepared films, because it is responsible for the variation of the crystal structure of the material that affects the physical properties of the materials.

c) Spraying Rate

Sprayer rate might cause a significant decrease in substrate temperature and lead to substrate crush. This parameter affects the homogeneity and thickness of the prepared films. In this study the spraying rate of the films was kept at (5 ml/min) to ensure a good stoichiometry and obtain a homogenous film.

d) Spraying Time

It is important to control the time period between every spraying operation, it should be uniform, and the spraying time period was 10 sec with 2 minutes wait between any two successive sprayings.

e) Distance « Nozzle from the substrate »

To obtain uniform film it is important to check the distance from the end of the capillary tube to the substrate is. In the present experiment the distance was fix it at 24 cm. Different distance causes scattering of the atomized solution away from the substrate, also any decrease in this distance will cause the collection of solution drops in one spot and this will affect film homogeneity.

f) The Drops Size Effect

The best deposition processes depend on the size of drops. The drops size effect on the preparation of obtains homogenous thin films. We have three Cases as we show in figure II.13 [75]:

Case A:

In this case, the drops size is large; therefore, the absorbed heat is not enough for solution evaporation. So, when the drop collides with the substrate it produces solid precipitate after solvent evaporation with a high decreasing rate in substrate temperature which causes the formation of inner potentials and leads to obtain a heterogeneous thin film and this affects the physical properties of the thin film.

Case B:

This represents the chemical spray pyrolysis operation, which gives the perfect properties for the thin film. In this case, the fine drops will evaporate in a short time before they reach the substrate, i.e. the particles reach the heated substrate as vapor phase, thus it can get enough heat to elevate its temperature, and therefore, the reaction on the substrate will take place.

Case C:

In this case, the drops are dried before they reach the substrate and become as powder on the substrate, which is distributed and condensed as smooth Grains on the substrate surface, it can easily be removed because its adhesion to the substrate is weak, this case happens when the spray distance is large.

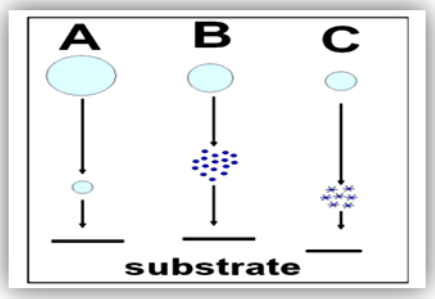

Figure II.13: The drops size effect [75].

II.3.Part B: Characterization techniques

In the following table, we cite some techniques for characterizing thin layers [76 - 77]:

Table II.3: Represents some techniques for characterizing thin layers.

Structural Characterizations				
Technique of Characterization	**Particles**	**Particles detected**	**Acronym**	**Information obtained**
Transmission Electron Microscopy	Electrons	Electrons	TEM	Thin film morphology
Scanning Electron Microscopy	Electrons	Secondary and backscattered electrons	SEM	Thin film morphology
Auger Microscopy	Electrons	Auger electrons	AM	Semi-quantitative analysis of the chemical composition and homogeneity of the latter as a function of the thickness of the layer

Tunneling Microscopy	Electrons	Electrons	TM	Morphology and density of electronic states of conductive or semiconductor surfaces
Spectroscopy Raman	Photons	Molecular Vibrations	SR	Structural information
Diffraction of X-rays	Photons x	Photons	XRD	* Degree of crystallization of thin layers and identification of the phases present * Determination of grain size, constraints ...
Spectroscopy of Photoelectrons	Photons x	Photoelectrons	SP	Chemical analysis

Optical characterizations and thickness measurement				
Technique of Characterization	**Particles**	**Particles detected**	**Acronym**	**Information obtained**
UV-visible Spectrophotometer	UV-visible Photons	UV-visible Photons	UVS	* Measurement of transmittance * Determination of the optical gap, urbach parameter, etc.
Ellipsometry	Visibles Photons	Change of Polarization	EM	Determination of thickness and refractive indices
Profilometer	Mechanical Tip	Point Jump	PM	Determination of layer thickness

➢ The techniques used for the characterization of the thin layers produced are:

✓ X-ray diffraction (XRD): for the study of structural properties.

✓ The UV-visible Spectrophotometer: for the study of optical properties.

✓ The four-point Technique: for the study of electrical properties.

✓ Weight difference method.

II.3.1 Structural characterization:

II.3.1.1 X-ray diffraction (XRD)

X-ray diffract meter is a powerful system for the study of nanostructure films since it gives a more information such as crystal structure, composition, and defects in the films. It is a nondestructive technique and does not need any specific sample preparation methods; the schematic diagram of the device is represented in the figure II.14. X-ray diffraction is founded on the constructive interference of monochromatic X-rays caused by crystalline materials. The cathode ray tube is responsible to produce X-rays and by a filtered to produce monochromatic radiation collimated to focus and directed across the sample. Crystals which can consider as the uniform arrangement of atoms; however X-rays can be treated as electromagnetic waves radiation. Atoms disperse X-ray waves, firstly through their electrons. X-ray striking an electron produces secondary spherical waves emanating from the electron. This physical phenomenon is well-known as elastic scattering, and the electron is known as the scattered [78].

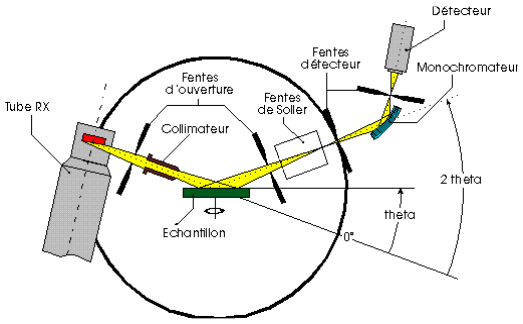

Figure II.14: Schematic diagram of X-ray diffract meter [79].

As part of our study, were used, Bruker - AXS D8 kind, X-rays were generated from a source Cu radiation having a wavelength of 1.541838 Å, with an acceleration voltage of 30 kV and a current of 40 mA. X-ray diffraction can be used to study the crystallographic properties of the thin films prepared such as determine of the crystalline structure, the orientation of the crystallites in a sample, the crystalline quality and the crystallite sizes.

Over the destructive interference, X-ray waves eliminate one another out in most directions, in a few particular directions constructive wave was added, determined by Bragg's law:

$$N\lambda = 2d_{hkl} \sin(\theta_{hkl}) \qquad \text{(II.3)}$$

Where:

N: is an integer. Waves that satisfy this condition interfere constructively and result in a reflected wave of significant intensity, figure II.15.

λ: is the wave length of the X-ray beam.

d_{hkl}: is the spacing between the parallel planes in the atomic lattice.

hkl: are the miller indices of the corresponding lattice planes (hkl).

θ_{hkl}: is the angel between the incident ray and the scattering planes.

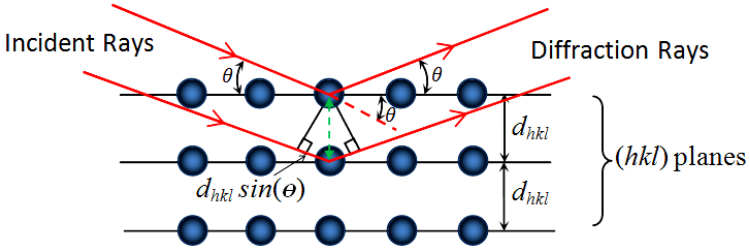

Figure II.15: Schematic of X-ray diffraction according to Bragg.

❖ **Information collected from the X-ray diffractogram:**

There is much information that we can deduce from the X-ray diffractogram, some of which are presented below:

II.3.1.1.1 Identification of phases

Identification of phases can be obtained in the following way: The comparison of observed d-values with standard d-values from international American Standard for Testing of Materials (ASTM) standard data file or Joint Committee for Powder Diffraction Standards (JCPDS) data file, for the same material synthesized by the standard chemical method. This analysis reveals the different phases appear in the film and Miller indices of the atomic planes. The lattice parameters for the unit cell of the phase present are calculated using equations given by Bragg´s law. The absence of reflection peaks indicates amorphous nature of the film [80].

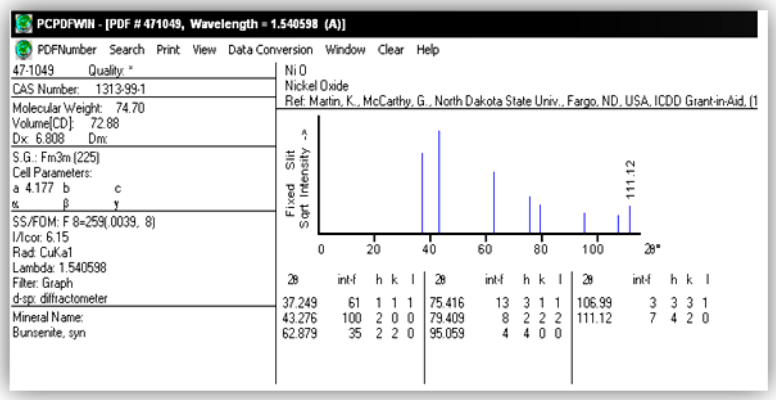

Figure II.16: JCPDS cards of NiO [81].

II.3.1.1.2 Inter-planar spacing

Inter-planar spacing was calculated from X-ray diffraction profiles using the formulaII.3.Using d values, the series of lattice planes (hkl) were identified from standard data. Strong peaks are expected when the condition of Bragg is satisfied. The lattice parameter values for different crystallographic systems can be determined from the following equations [82]:

- For the cubic systems**:** $\frac{1}{d^2} = \frac{h^2 + k^2 + l^2}{a^2}$ (II.4)

II.3.1.1.3 Crystallite size (Grain size)

The crystallite or grain size of samples can be established by the Scherer formula:

$$D_{hkl} = \frac{0.9\,\lambda}{\beta_{hkl}\,Cos\,(\theta_{hkl})} \quad \text{(II.5)}$$

Where:

D_{hkl}: is the average grain size obtaining from the peak (hk1).

λ: is the wavelength applied for X-ray of (λ= 1.5406 Å).

β_{hkl}: is the full width at half maximum intensity of the peak (hk1).

θ_{hkl}: is the angel between the incident ray and the (hk1) scattering planes.

II.3.1.1.4 The texture coefficient

The texture coefficient T_c illustrates the texture (the distribution of crystallographic orientations of a polycrystalline sample) of the specific plane, deviation of which from unity reveals the preferred growth. About the preferential orientation quantitative information was effectuated from the different texture coefficient $T_{c\,(hkl)}$ defined as [81]:

$$T_{C(hkl)} = \frac{\frac{I\,(hkl)}{I_0\,(hkl)}}{1/N \sum \frac{I\,(hkl)}{I_0\,(hkl)}} \quad \text{(II.6)}$$

Where:

I (hk1): is the relative experimental intensity from (hk1) plane,I_0 (hk1)is the intensity of standard pattern from the JCPDS information and N is the reflection number.

II.3.1.1.5 Microstrain

The line varying experimental XRD patterns from that of the standard patterns indicate the strain developed throughout the synthesis of the films. Microstrain was calculated by using equation II.7 [82]:

$$\varepsilon = \left[\frac{a - a_0}{a_0}\right] \times 100 \quad \text{(II.7)}$$

Where:

ε: is the mean strain, a: is the calculated lattice constant thin films and a_0: the standard lattice constant of bulk material according to standard card (JCPDS).

II.3.1.1.6 Dislocation density and Number of Grains

The defects quantity in the material was determined by calculating the dislocation density δ from the following formula [82]:

$$\delta = \frac{1}{D_{av}^{\ 2}}$$

(II.8)

Where: D_{av} is the crystallite size.

And number of crystallites can be calculated from the relation [83]:

$$N_0 = t/D_{av^2} \qquad \text{(II.9)}$$

Where:

t: is the thickness and N_0: is the number of crystallites.

II.3.2 Optical characterization:

Spectrophotometers are optical devices that determine the light intensity of reflected or transmitted using objects with a variation of wavelength. Light throughout the lamp enters the monochromator, which makes the light dispersion and selects the particular wavelength chosen by the operator for the measurement. After that, the chosen wavelength is moved alternately throughout the sample and along the reference path. The reference and sample light beams pass via the cell compartment, consisting of a reference space and a sample space. The two light beams converge on the detector. Transmittance or absorbance of solid or liquid and total diffuse reflectance/transmittance of solids like large disks, silicon wafers, plastics, glass etc. can be measured. Band gap determination, electron transition and enzyme activity studies can also be made.

A diagram of the typical constituent of the spectrophotometer is represented from the figure II.17 by using diffraction grating or prism the beam of light (visible or/and UV light source) is divided, into its component wavelengths. The beam intensity (reference beam) defined as I0, which becomes small or no light absorption. However the beam intensity of the sample defined as I. Over a short period of time, automatically the spectrometer sweeps all the component wavelengths from the previous description. The ultraviolet (UV) portion is studied from 200 to 400 nm, and the visible section is ranged in 400-800 nm. If the sample does not absorb light of a given wavelength, I=I0. Furthermore, if the sample absorbs light then I is less than I0, and this variation may be plotted on a graph versus wavelength. Absorption was

displayed as transmittance (T = I/I0) or absorbance (A= log I0/I). If no existence of absorption so T = 1.0 and *A*= 0 [84].

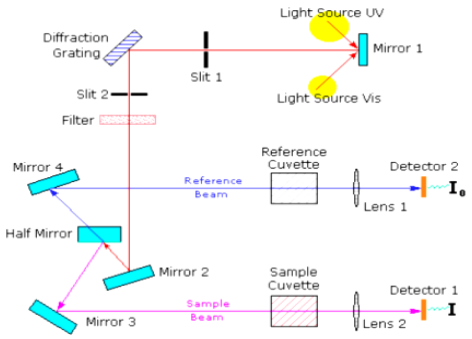

Figure II.17: Schematic representation of UV-visible spectrometer [85].

❖ **Information obtained from the UV-visible transmittance spectra:**

Much information is obtained about the properties of materials when they interact with electromagnetic radiation. When the light beam (photons) is an accident on an object, there is some expected absorption, determined by the properties of the material. In the following we will integrate the properties of films that can be deduced from the transmittance spectrum.

II.3.2.1 Absorption coefficient

An electronic transition between the conduction and valence bands in the crystal starts at absorption edge which equals to the least energy variation between the highest maximum of the valence band and the lowest minimum of the conduction band. If these extreme lie at the similar point of the k-space then the transition is called direct. If this is not, then only phonon assisted transitions called indirect transitions are possible as depicted in figure II.18. Optical absorption of materials is directly allied with the coefficient of absorption α. It is crucial to determine the absorption characteristics of glasses and thin films, especially when comes to optical materials is subject to exploit their applications possibilities. When light is incident on thin films some of its energy is reflected, some is absorbed and rest is transmitted. The optical absorption in thin films depends on thickness and wavelength and is a function of its structural properties. From the transmission spectra, the coefficient of absorption values was established by the Beer-Lambert Law [86]:

$$\alpha = {}^{1}/_{t}\, ln\left(\frac{1}{T}\right) \qquad \text{(II.10)}$$

Where:

T is the transmittance and t is the sample thickness .The reliance of absorption coefficient on photon energy in the high absorption regions is achieved to get more information concerning gap energy.

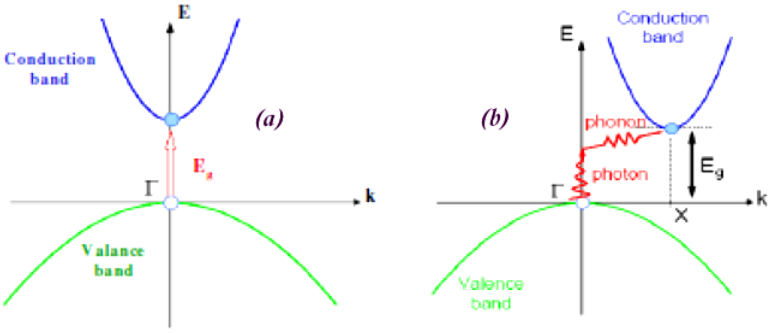

Figure II.18: E-K diagram showing (a) direct band and (b) indirect band transition [87].

II.3.2.2 Optical band gap energy

The optical gap energy is one of the fundamental characteristics of optical materials. The measurement of gap energy relies not only on the material but also on its characteristics and stoichiometry. The energy limited to the highest maximum of the band of valence the and lowest minimum of the band of conduction is known as band gap energy (Eg). By determination of the absorption coefficient values, Eg value can be evaluated by the Tauc's formula [86]:

$$(\alpha h\nu) = B\,(h\nu - E_g)^{n} \qquad \text{(II.11)}$$

Where:

B: is a constant which does not correlate to the photon energy, α :is the absorption coefficient, (hν): is the photon energy and n is an index that indicates the optical absorption mechanism and it is equivalent to 3, 2,3/2, and 1/2 when the transition is indirect forbidden, indirect allowed, direct forbidden and direct allowed, respectively.

Direct band gap was evaluated using extrapolating the straight-line portion $(\alpha h\nu)^2$ as a function of (hν) to the energy axis at zero absorption coefficient (α=0) as observed from figure II.19.

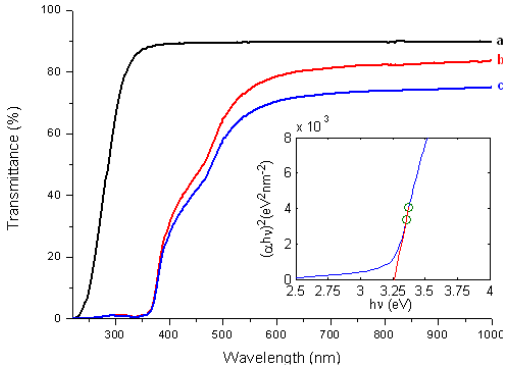

Figure II.19: The curve of (αhν) ² as a function of the incident photon energy (hν) to calculate the band gap [88].

II.3.2.3 Urbach Energy

Generally, in optical absorption, close band edges, an electron from the top of the valence band get excited into the bottom of the conduction band across the energy band gap. During this transition process, if these electrons happen disorder, it causes the density of their states ρ (hν), where hν is the photon energy, tailing into the energy gap. This tail of ρ (hν) extending into the gap energy is termed as Urbach tail as shown in figure II.19.

Consequently, absorption coefficient α (hν) also tails off in an exponential mode and the Energy-related with this tail is referred to as Urbach energy and can be calculated by the Following equation:

$$\alpha\ (h\nu) = \alpha_0 e^{\frac{h\nu}{Eu}} \qquad \text{(II.12)}$$

Where:

α_0: a constant, hν is the photon energy and Eu is the Urbach energy. The Eu energy is determined using the plotting ln (α) vs. hν and fitting the linear part of the curve with a straight line .From the linear region of reciprocal of the slope give up the Eu value. The Eu values of the samples, which decreases in the case of crystallization at higher temperatures.

Because Urbach energy of glassy semiconductors fundamentally defines the disorder level, crystallization and resulted order of this process decrease the Eu in value [89].

The gap energy was drawn from the Tauc relation by plotting the graphical representation (αhν) ² as a function of (hν) figure II.20.

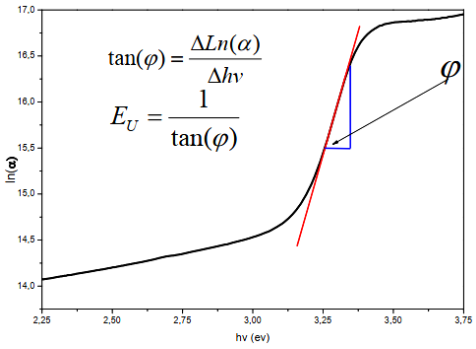

Figure II.20: Determination of Urbach energy of the layer [90].

II.3.3 Electrical characterization

II.3.3.1 The four-point method

Four-point probe (4PP) systems measure sheet resistance (R_s), the local resistance of a sheet of material, in units of ohms/square. Sheet resistance is expressed in the equation $R_s = R_b/t$, where t is the thickness of the conductive layer, and R_b is the bulk resistivity (ohm-cm) of the layer. For a material with constant bulk resistivity, the sheet resistance is only a function of thickness. A four-point probe consists of four spring-loaded conductive probes (usually in a linear array) which are placed in contact with the material whose sheet resistance is to be measured. (The four-point probe technique requires some isolating junction or blocking layer to the DC current used). Typically, a known current is forced between the outer probes, and the resulting voltage across the inner two is measured. Ohm's Law (V = IR) is then used, with a geometrical correction factor, to calculate the sheet resistance of the material. To compensate for geometric errors arising from variations in probe tip spacing and proximity to the wafer edge, the dual configuration technique was developed. A second measurement is made, with current forced through pins 1 and 3, and voltage measured between pins 2 and 4 (figure II.21). The geometrical correction factor can then be calculated Based on the ratio of the measured resistivity [91].

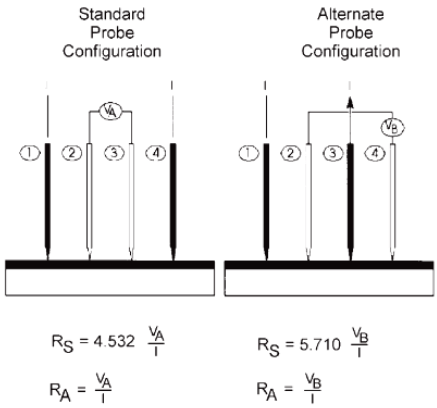

Figure II.21: Dual configuration four-point probe measurement setup.

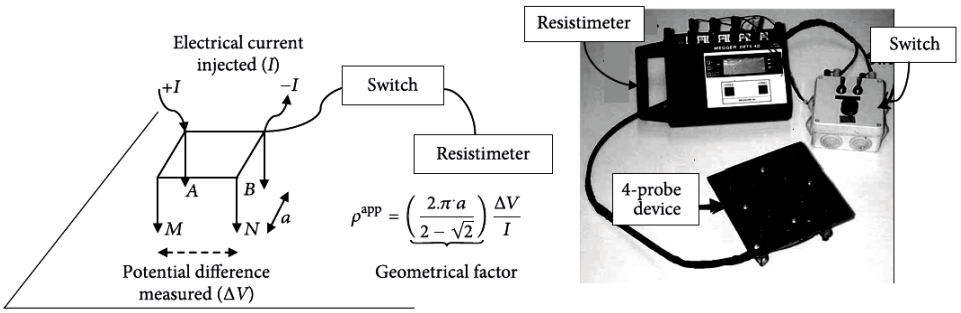

Figure II.22: Four-probe square array principle [91].

II.3.4 Weight difference method (thickness measurement):

Thickness is one of the most important thin film parameters since it largely determines the properties of the film. The thickness of the films is usually measured by monitoring the rate of the deposition during the coating process. However there are several methods used for measuring thickness of the film, such as gravimetric, optical, electrical and other methods. In the current experiment the thickness of the thin films was measured by the gravimetric method.

II.3.4.1 The gravimetric method

This method is done by using sensitive electronic balance with four digits sensitivity (10^4g). The substrates are weighted before and after deposition. From the weight difference and the area of substrate, the thin film thickness (t) can be measured, according to the following equation [92]:

$$T = \Delta m / \rho_0 \times A_S \qquad \text{(II.13)}$$

Where:

Δm: is the weight difference of substrate. This means that it is the mass of the thin film (g).

A_S: area of the thin film Cm^2, ρ_0: the density of material of the thin film (6.67 g/ Cm^3) for nickel oxide and (6.45 g/Cm^3) for cobalt, the density of material calculated from:

*Total density (ρ_0) = density of NiO × its percentage in the solution + density of CO × its percentage in the solution. (II.14)

II.4 Conclusion

In this chapter we have presented in the Part A; the experimental methodology of our work like preparation of chemical base solution and it's mixing with different doping percentage which deposited by spray pyrolysis technique. Where part B we are also presented some different analysis technique used in our characterization study, namely X-ray diffraction (XRD), Spectroscopy (UV-Vis), four-point resistivity and weight difference methods.

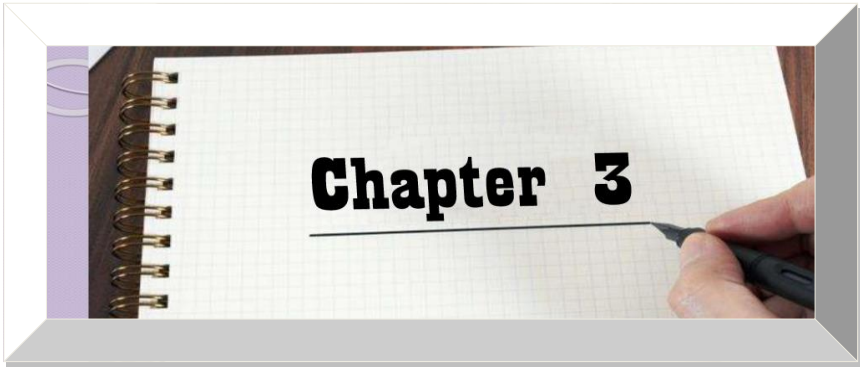
Chapter 3


Results

Results :

III.1 Image of thin films

Figure III.1 shows the photo image of Nickel-Cobalt Oxide thin films, where x = 0, 1.5, 3, 4.5, 6 and 7.5 %. It is reported that the stoichiometrically correct NiO thin films are expected to have green color; however, the non-doped NiO thin film deposited in the present study has black-grey color which can be attributed to non-stoichiometry of the deposited material. It can also be observed that the Co-doped NiO thin films are accompanied by a color change from black to orange. This change of color is attributed to the Cobalt doping.

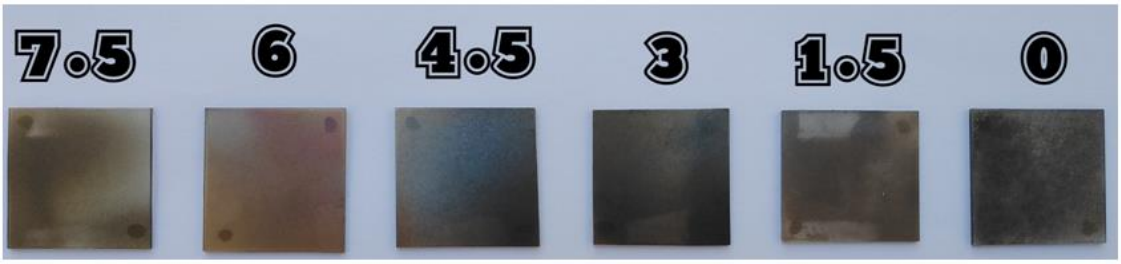

Figure III.1: Photo image of ($Ni_{(1-x)}Co_xO$) thin films, where x = 0, 1.5, 3, 4.5, 6 and 7.5 %.

III.2 Optic characteristic:

III.2.1 Transmittance spectrum

Figure III.2 shows the transmission and absorption spectra of the sprayed NiO: CO thin films in the wavelength range of 300-1100 nm. It is observed that the transmission is about 22-50 % in the visible range and it increases to the maximum which is 60 % in the infrared domain for the percentage of Cobalt of 6 %.

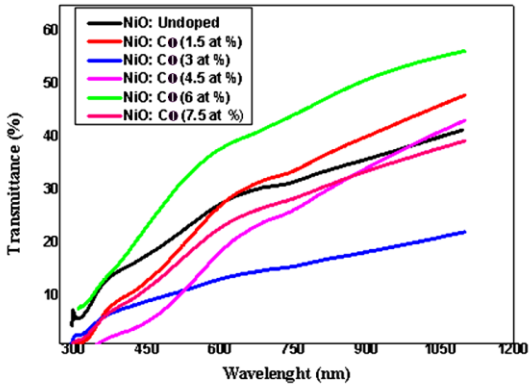

Figure III.2: Transmission spectra for non-doped and CO-doped (1.5, 3, 4.5, 6 and 7.5 %) NiO films prepared at 450 °C.

III.2.2 Gap energy (Eg)

From figure III.3, the band gap values are determined as a function of Cobalt concentrations by extrapolating the straight line portion of the $(\alpha h\nu)^2$ versus $(h\nu)$ variation to $(\alpha h\nu)^2 = 0$. The values were collected in the table III.1.

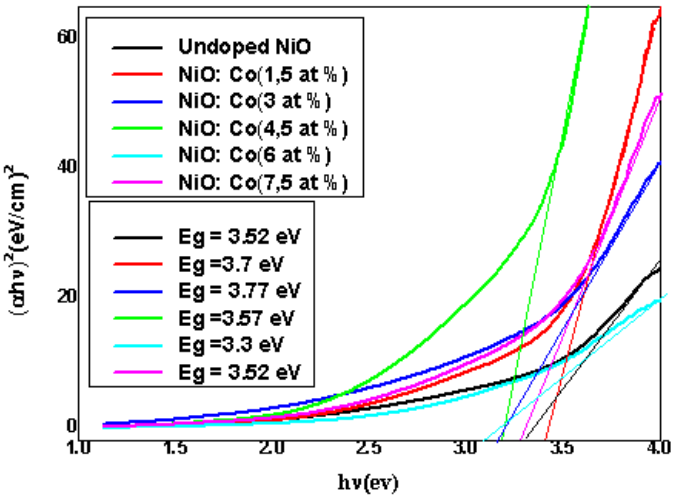

Figure III.3: Plots of $(\alpha h\nu)^2$ versus $h\nu$ for NiO: Co films with different values of Cobalt concentration.

Table III.1: Gap energy values.

Co %	0	1.5	3	4.5	6	7.5
Eg (eV)	3.52	3.7	3.77	3.57	3.3	3.52

Results of previous works

III. 3 First previous work:

This work was performed to elaborate and characterize thin films of NiO: Co deposited on glass substrate at 350 °C, with different percentage of doping (3 % .6 %. 9 % and 12 %). These conditions were very close to our experimental conditions. Thus the results obtained in this case will be studied as an important previous work.

III.3.1 Structural characterization:

III.3.1.1 X-ray diffraction

XRD patterns have shown that both non-doped and Co-doped NiO thin films exhibit the cubic crystal structure with a preferential orientation along [111] direction.

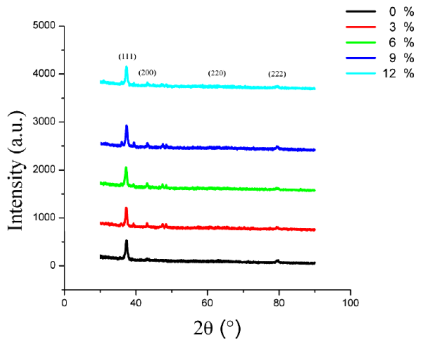

Figure III.4: X ray diffraction spectrum of non-doped thin layers and doped NiO: Co [93].

III.3.1.2 Grain size

It was observed in figure III.5 that the crystallite size for the oxide films of doped Nickel Cobalt increases with the increase in the percentage of Cobalt from 0 - 9% to reach a maximum value of 31.86 nm, then it decreases to 19.26 nm for the percentage of Cobalt of 12% which is in agreement with the results of other authors.

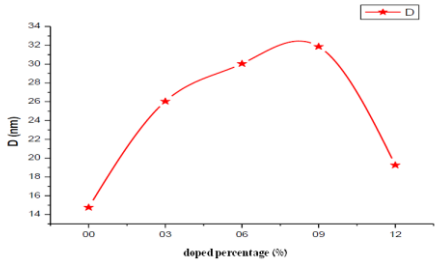

Figure III.5: Grain size of thin layers of pure and doped Nickel Oxide Cobalt [93].

III.3.2 Optic characteristic:

III.3.2.1 Transmittance spectrum

It has been observed that the transmittance increases with the wavelength of the spectrum shows a weak transmittance in the ultraviolet domain, a transmittance of 20 % -50 % in the visible range and it increases to the maximum which is 60 % in the infrared domain, for the percentage of Cobalt of 6 %.

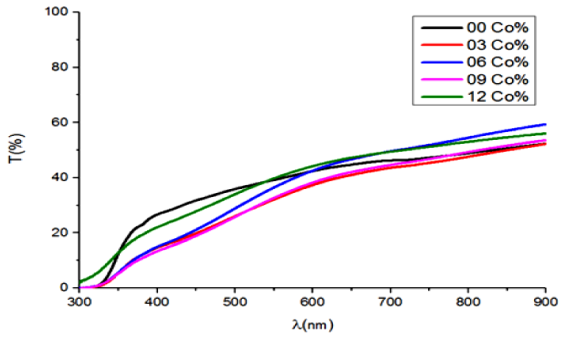

Figure III.6: Transmittance spectra for thin oxide layers pure Nickel and Cobalt doped [93].

III.3.2.2 Gap energy (Eg)

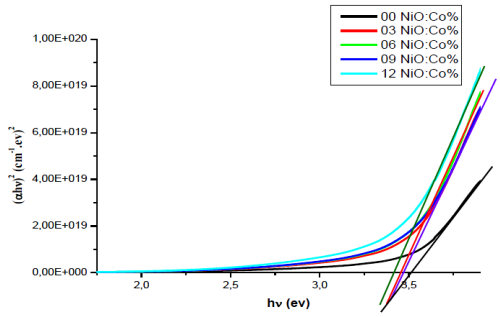

Figure III.7: Plots of $(\alpha h\nu)^2$ versus hν for NiO: Co films with different values of Cobalt concentration [93].

Table III.2: Gap energy values.

Co %	0	3	6	9	12
Eg (eV)	3.50	3.47	3.47	3.45	3.43

III.3.2.3 Urbach energy (Eu)

Table III.3: Urbach energy values.

Co %	0	3	6	9	12
Eu (meV)	461.9	540.5	560.7	638.6	710.0

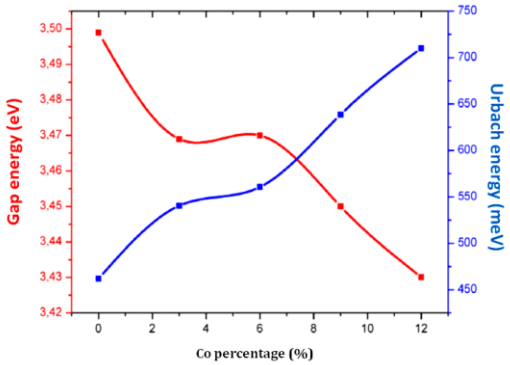

Figure III.8: Variation of the optical Gap and Urbach energy of NiO: Co films versus doping percentage [93].

III.3.3 Electrical conductivity:

The best value of the electrical conductivity is 7.29 x 10^{-6} $(\Omega.cm)^{-1}$ was obtained for 3 at % Co doping.

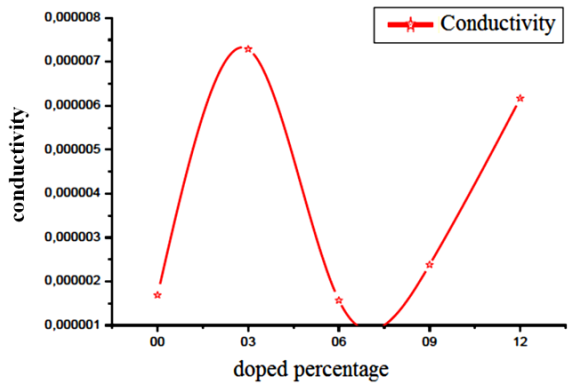

Figure III.9: The electrical conductivity of NiO: Co films deposited versus doping percentage [93].

III.3.4 Conclusion:

The average optical transmittance for NiO is above 50 % in the visible region, and it reduces for NiO-CO thin films. Whereas the optical band gap value decreases from 3.77 to 3.3 eV as doping concentration increases.

For the previous works we have recorded the fellow results:

- X-ray diffraction spectrum have shown that the structure of thin layers of Cobalt doped Nickel Oxide that we developed is a structure crystallized, the peaks appear at $2\theta \approx 37$ ° with a preferential orientation according to the plane (111) which indicates that these layers crystallize in the cubic structure.
- The transmittance between 50 and 60 % in the visible and infrared range, which proves that the layer transmits light in these areas.
- The best conductivity is that which was obtained for the layer of Nickel Oxide doped with 3 % Cobalt, it is around 7.29 10^{-6} (Ω.cm) $^{-1}$, the other conductivity values, for other Cobalt percentages, are included between 1.5710^{-6} and 7.29 10^{-6} (Ωcm) $^{-1}$, and the best conductivity was obtained for the layer of Nickel Oxide doped with 3 % Cobalt**.**

III.4 Second previous work:

The effect of Co doping on structural and optical properties of NiO thin films prepared by chemical spray pyrolysis method.

In this work, Nickel-Cobalt Oxide ($Ni_{(1-x)}Co_xO$) thin films, where x = 0, 4, 6 and 8 % have been successfully deposited on glass substrates by chemical spray pyrolysis (SPT) technique at substrate temperature of (400 °C) and thickness of about 300 nm.

III.4.1 Structural analysis:

III.4.1.1 X-ray diffraction

XRD patterns of the Co-doped Nickel Oxide films are shown in figure III.10. It can be noticed that all the patterns exhibit diffraction peaks around (2θ~37°, 43° and 63°) referred to (111), (200) and (220) favorite directions respectively. The strongest peak occurs at 2θ~37° which is referred to (111) plane. The positions of the peaks and the presence of more than one diffraction peak lead to the conclusion that the films are polycrystalline in nature with a cubic crystalline-structure.

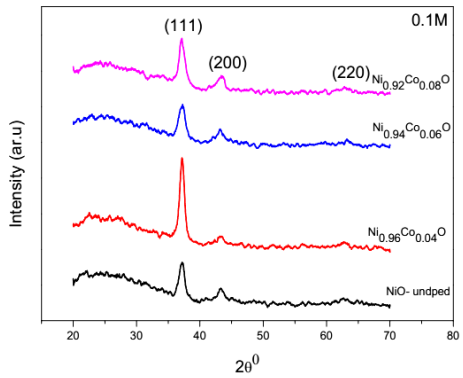

Figure III.10: XRD patterns of Co-doped Nickel Oxide thin films [94].

III.4.1.2 Grain size

It is observed that the crystallite size for the Nickel-Cobalt Oxide thin films decrease rapidly as the Co-concentration increases from 0 to 0.04 to reach its minimum value of (8.22 nm). The crystallite size then increases as the Co-concentration increases further to reach value of (10.1 nm) as shown in figure III.11.

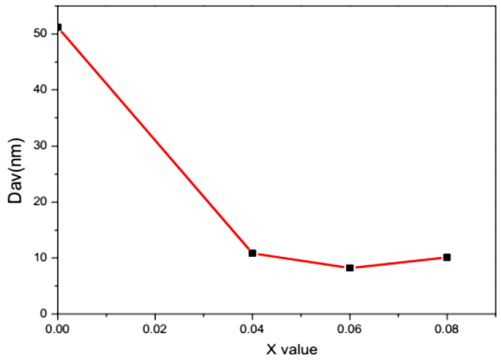

Figure III.11: The crystallite size of Nickel-Cobalt Oxide thin films [94].

III.4.2 Optical analysis:

III.4.2.1 Transmittance

Optical absorption spectra of the films in spectral range of (300-900 nm) were recorded by using UV–visible spectrophotometer. Figure III.12 shows the relation between transmittance and wavelength for Co-doped Nickel Oxide thin films. It can be noticed that the transmittance increases rapidly as the wavelength increases in the range of (300- 350 nm), and then increases slowly at higher wavelengths. The spectrum shows high transmittance in the visible and infrared regions, and low in the ultraviolet region.

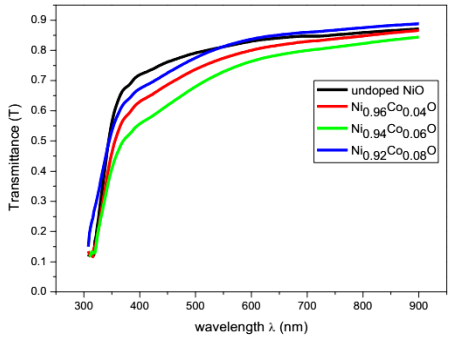

Figure III.12: Transmittance (T) versus wavelength (λ) for Co- doped Nickel Oxide thin films [94].

III.4.2.2 Gap energy (Eg)

It’s noticed that the band gap value decreases with increase in Co-doping concentration (4, 6, and 8) wt. % (figure III.11).

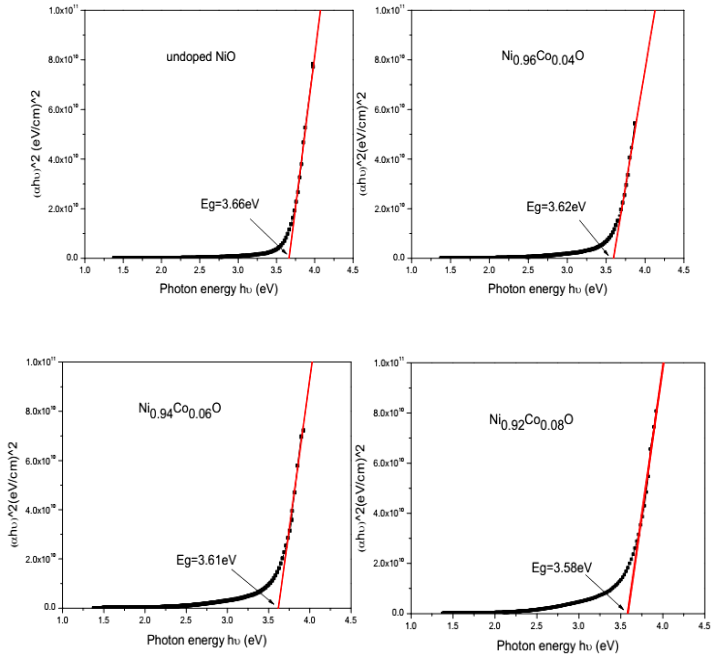

Figure III.13: The relation between $(\alpha h\nu)^2$ and (hυ) for Co-doped Nickel Oxide thin films [94].

III.4.2.3 Urbach energy (Eu)

Urbach energy increases with increase in Co-doping concentration. The Eu values change inversely with optical band gaps of films (figure III.14).

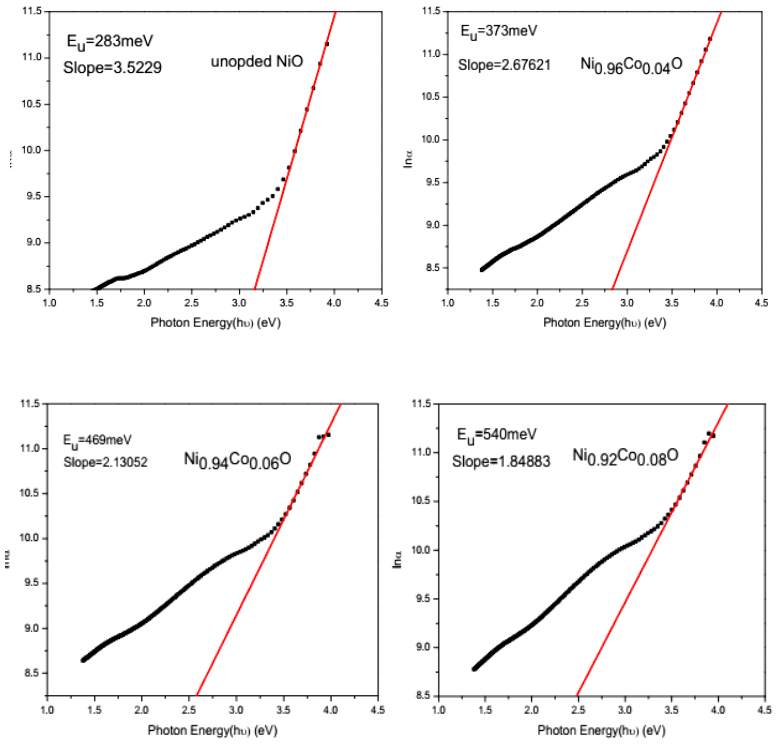

Figure III.14: Urbach plots of co-doped Nickel Oxide thin films [94].

III.4.3 Conclusion:

In this study Nickel-Cobalt Oxide ($Ni_{(1-x)}Co_xO$) thin films, where x = 0, 4, 6 and 8 % were successfully deposited on glass substrate at (400 ºC) by chemical spray pyrolysis technique using Nickel and Cobalt Nitrates as the Ni and Co source.

- XRD patterns of the Co doped Nickel Oxide thin films indicate that all films are polycrystalline with cubic face centered crystal structure.
- The non-doped NiO thin film has highest grain size.
- The transmittance of Co doped Nickel Oxide thin films increases rapidly as the wavelength increases in the range of (300-350) nm, and then increases slowly at higher wavelengths.
- The band gap decreases as the Co-concentration increases and the band gap values range between 3.66 eV and 3.58 eV.
- The Urbach energy increases as the Co-concentration increases and the Urbach energy values range between 283 meV and 540 meV.

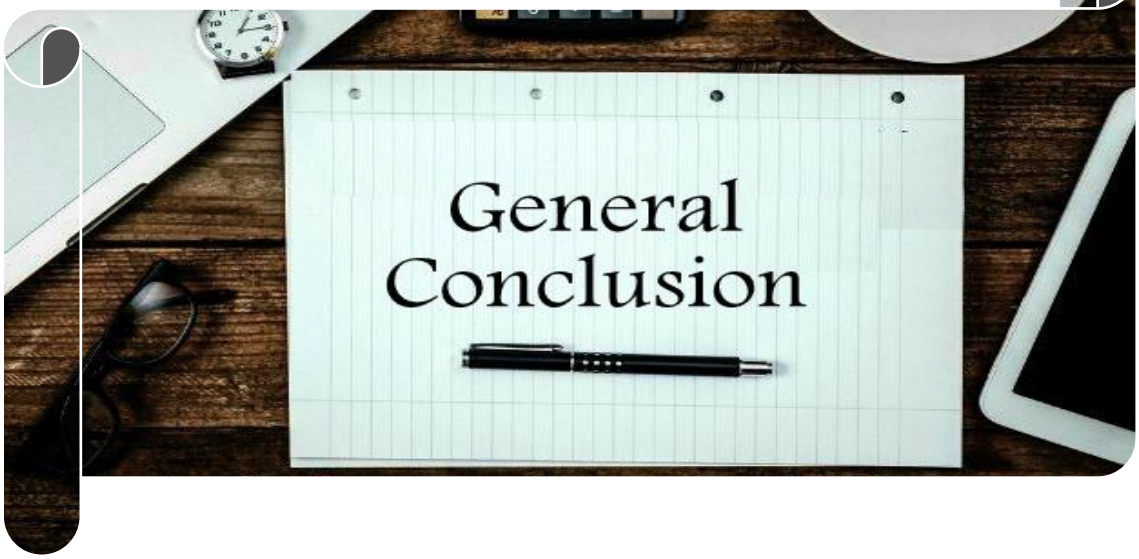
General
Conclusion

General Conclusion

Nickel Oxide (NiO) is a promising semiconductor material. Our interest in Nickel Oxide thin films was due to its outstanding properties and their importance in many applications in science and technology. In this work, we have prepared samples of thin layers of Nickel Oxide, which have been doped with different percentages of Cobalt (1.5, 3, 4.5, 6 and 7.5 %), where we have deposited these layers on glass substrate at 450 ^{o}C by spray pyrolysis technique (SPT).

The aim of this work is to study the effect of doping of Nickel Oxide by Cobalt on the structural, optical and electrical properties. To characterize these samples, we have to use several techniques, such as X-ray diffraction for structural characterization, UV-Visible spectroscopy for optical characterization, the four-point method for electrical characterization and weight difference methods for thickness measurement. Unfortunately the sanitary situation for this school year doesn't allow the practice of these techniques. Thus we have studied some of previous works related to our work.

The results collected from this study are:

The transmission and absorption spectra of the sprayed NiO-CO thin films in the wavelength range of 300-1100 nm. It is observed that the transmission is about 22-50 % in the visible range and it increases to the maximum which is 60 % in the infrared domain for the percentage of Cobalt of 6 %. Whereas the optical band gap value decreases from 3.77 to 3.3 eV as doping concentration increases.

The most important results summarized from these previous works were as follow:

- That all XRD patterns of the Co doped Nickel Oxide thin films indicated that all films are polycrystalline with cubic face centered crystal structure and the crystallites adopt a preferential orientation in the direction (111). Also all thin films studied shown that the non-doped NiO thin film has highest grain size.
- The transmittance of Co doped Nickel Oxide thin films increases rapidly as the wavelength increases in the range of (300-350) nm, and then increases slowly at higher wavelengths.
- For the both studies, we have noticed that the band gap decreases as the Cobalt concentration increases. Whereas the Urbach energy increases as the Co-concentration increases.

Abstract:

In this work, we have prepared thin film of non-doped and doped Nickel Oxide (Cobalt) from Nickel Nitrate Hex-hydrate ($Ni\ (NO_3)_2.6H_2$), Chloride of Cobalt ($CoCl_26H_2$) at different concentrations (0 %, 1.5 %, 3 %, 4.5 % and 7.5 %). Other parameters was fixed such as the substrate temperature (T = 450°C), the deposition time (25 min), the nozzle-substrate distance (24 cm), the molarities of the solution (0.1 mol / l) and the pressure spraying (2 bar). The deposit is made on a glass substrate by the pyrolysis spray technique.

The results collected from this study are:

The transmission and absorption spectra of the sprayed NiO-CO thin films in the wavelength range of 300-1100 nm. It is observed that the transmission is about 22-50 % in the visible range and it increases to the maximum which is 60 % in the infrared domain for the percentage of cobalt of 6 %. Whereas the optical band gap value decreases from 3.77 to 3.3 eV as doping concentration increases.

The results of previous works studied shown:

- That all XRD patterns of the Co doped Nickel Oxide thin films indicated that all films are polycrystalline with cubic face centered crystal structure and the crystallites adopt a preferential orientation in the direction (111). Also all thin films studied shown that the non-doped NiO thin film has highest grain size.
- The transmittance of Co doped Nickel Oxide thin films increases rapidly as the wavelength increases in the range of (300-350) nm, and then increases slowly at higher wavelengths.
- For the both studies, we have noticed that the band gap decreases as the Co-concentration increases. Whereas the Urbach energy increases as the Co-concentration increases.

ملخص:

في هذا العمل قمنا بتحضير طبقات رقيقة من أكسيد النيكل غير مطعمة و مطعمة بعنصر (كوبالت) انطلاقا من نيترات النيكل ($Ni(NO_3)_2.6H_2O$)، كلوريد الكوبالت ($CoCl_26H_2$) بتراكيز متغيرة للكوبالت (0 %، 1.5%، 3 %، 4.5 %، 6 %، 7.5 %) مع تثبيت الخصائص الأخرى حيث درجة حرارة المسند (450 درجة مئوية)، ومدة التوضع (25 دقيقة)، المسافة بين المرذاذ و المسند (24 سم)، مولارية المحلول (0.1 مول / لتر)، وضغط الرش (2 بار) و التوضع يكون فوق ركائز زجاجية بواسطة طريقة الرش مع الانحلال الحراري.

النتائج التي تم جمعها من هذه الدراسة هي:

أطياف النقل والامتصاص للأغشية الرقيقة NiO-CO في نطاق الطول الموجي 300-1100 نانومتر. ويلاحظ أن النفاثية حوالي 22-50٪ في المدى المرئي ويزيد إلى الحد الأقصى وهو 60٪ في مجال الأشعة تحت الحمراء لنسبة الكوبالت التي تبلغ 6٪. في حين أن قيمة فجوة النطاق البصري تنخفض من 3.77 إلى 3.3 eV مع زيادة تركيز المنشطات.

ظهرت نتائج الأعمال السابقة التي تمت دراستها ما يلي:

- أظهرت نتائج فحوصات الأشعة السينية أن الشرائح غير مطعمة و مطعمة المحصل عليها تتبلور وفق بنية مكعبة . الحبيبات المكونة للشرائح الرقيقة لها توجه مفضل وفق الاتجاه (111).
- كما أظهرت نتائج الفحص الشرائح الرقيقة التي تمت دراستها أن الشرائح الرقيقة الغير مطعمة لديها أكبر حجم حبيبي
- تزداد نفاذية الشرائح الرقيقة لأكسيد النيكل المطعمة ة بسرعة مع زيادة الطول الموجي في نطاق (300-350) نانومتر ، ثم تزداد ببطء عند أطوال موجة أعلى.
- في كلتا الدراستين ، لاحظنا أن فجوة النطاق تنخفض مع زيادة التركيز للكوبالت. في حين أن طاقة Urbach تزداد كلما زاد التركيز.

Résumé:

Dans ce travail, nous avons préparé des couches minces d'Oxyde de Nickel non dopée et dopée cobalt à partir du Nitrate de Nickel d'Hydraté $Ni(NO_3)_2.6H_2$, Chlorure de Cobalt ($CoCl_26H_2$) à différentes concentrations (0 %, 1.5 %, 3 %, 4.5 % et 7.5 %). Nous fixons les autres paramètres tels que la température du substrat (T = 450°C), le temps de dépôt (25 min), la distance bec-substrat (24 cm), la molarité de la solution (0.1 mol/l) et la pression de pulvérisation (2 bar). Le dépôt se fait sur un substrat de verre par la technique de spray pyrolyse.

Les résultats de cette étude sont les suivants :

Les spectres de transmission et d'absorption des films minces NiO-CO pulvérisés dans la gamme de longueurs d'onde de 300-1100 nm. On observe que la transmission est d'environ 22 à 50% dans le domaine visible et elle augmente au maximum qui est de 60% dans le domaine infrarouge pour un pourcentage de cobalt de 6%. Alors que la valeur de la bande interdite optique diminue de 3,77 à 3,3 eV à mesure que la concentration de dopage augmente.

Les résultats des études antérieurs montrent :

- Que tous les peaks du DRX des films minces d'Oxyde de Nickel Co dopés indiquaient que tous les films étaient polycristallins avec une structure cristalline cubique à face centrée les cristallites adoptent une orientation préférentielle suivant la direction (111).
- De plus, tous les films minces étudiés ont montré que les NiO non dopé ont la taille de grain la plus élevée.
- La transmittance des couches minces d'Oxyde de Nickel Co dopées augmente rapidement quand la longueur d'onde augmente dans la plage de (300-350) nm, puis augmente lentement à des longueurs d'onde plus élevées.
- Pour les deux études, nous avons remarqué que la bande interdite diminue à mesure que la Co-concentration augmente. Alors que l'énergie d'Urbach augmente à mesure que la Co-concentration augmente.


References

References

[1] J. L. Van Heerden and R. Swanepoel, Thin Solid Films 299, 72 (1997).

[2] C. H. Lee and L.Y. Lin, Appl. Surf. Sci. 92,163 (1996).

[3] C. Wang, Z. Ji, J Xi, J. Du, and Z. Ye, Materials Letters 60 (2006) 912- 914.

[4] S. Yahiaoui, The effect of the morality of the different sources of tin on the properties of the thin layers of tin oxide SnO2 produced by Ultrasonic Spray, Magister Theses, Biskra University, Algeria, (2014).

[5] D. Royer and E. Dieulesaint, "Elastic waves in solids (Generation, acousto-optic interaction, applications) ", Edition Masson, Tome 2, France, (1999).

[6] M. Boussafeur, Master thesis, Larbi Ben M ‟Hidi University Oum El-Bouaghi, (2012).

[7] J. Aronovich, A. Ortiz and R. H. Bube, J.Vac.Sci. Technol. 16.994 (1979).

[8] J. F. Chang, C. C. Shen and M. H. Hon, Ceramics Internet 29 (2003) 245.

[9] http://fr.wikipedia.org/wiki/couche_mince.57 .

[10] https://www.cefi.org (Fra DESS.old / dess_265 html).

[11] S. Yamaga, A. Yoshokawa, H. Kasain, Cryst. Growth 86 (1998) 250.

[12] I.C. Ndukwe, Sol. Energy Mater. Ground, Cells 40 (1996) 123.

[13] T.E. Varitimos, R.W. Tustison, thin Solid Films 151 (1987) 27.

[14] M. Doudi, N. Talebian, The study of antibacterial properties of NiO thin film using Sol gel Synthesis, Biological Forum-An International Journal, 8 1 (2016) 127-131.

[15] Q. Pan, J. Liu, Facile fabrication of porous NiO films for lithium-ion batteries with highreversibility and rate capability, J. Sol. St. Electrochemist., 13 10 (2009) 1591–1597.

[16] https://www.britannica.com/science/nickel-chemical-element.

[17] https://www.britannica.com/EBchecked/topic/414238/nickel-Ni

[18] Department of Health, Public Health Service.ATSDR, And Toxicological Profile for Nickel, Atlanta, GA, USA: US (2005).

[19] F. Ullmann Y. S. Yamamoto, F. T. Campbell, R. Pfefferkorn, J. F, Rounsaville-Ullmann ‟sencyclopedia of industrial chemistry. VCH (1996).

[20] P. Pradyot, Handbook of Inorganic Chemicals, McGraw-Hill, Publications, (2002).

[21] N.A. Bakr, S.A. Salman, A.M. Shano, Effect of Aqueous Solution Morality on Structural and Optical Properties of nickel oxide Thin Films Prepared by Chemical Spray Pyrolysis Technique, International Journal of Current Research, 41(2014)15-30.

[22] B. Sasi, Preparation and characterization studies of nanostructure nickel oxide and lithium doped nickel oxide thin films, PhD thesis, University of Kerala, 2007.

[23] Z. Zhiwei, Oxygen reduction on lithium nickel oxide as a catalyst and catalyst support, PhD thesis, Case Western Reserve University, 1993.

[24] A. M. Soleimanpour, Synthesis, fabrication and surface modification of monocrystalline nickel oxide for electronic gas sensors, PhD thesis, University of Toledo, 2013.

[25] H. A. Juybari, M.M. Bagheri-Mohagheghi, M. Shokooh-Saremi, Nickel–lithium oxide alloy transparent conducting films deposited by spray pyrolysis technique, Journal of Alloys and Compounds, 509 (2011) 2770-2775.

[26] A. Citra, G. V. Chertihin, L. Andrews, M. Neurock, Reactions of Laser-Ablated Nickel Atoms with Oxygen. Infrared Spectra and Density Functional Calculations of nickel oxides NiO, Ni_2O_2, and Ni2O3, Superoxide NiOO, Peroxide Ni(O2), and Higher Complexes in Solid Argon, The Journal of Physical Chemistry A, 101 (1997) 3109-3118.

[27] W.D. Callister, Fundamentals of materials science and engineering- An integrated approach. Second ed., USA: John Wiley & Sons, 2005.

[28] Wu. Hongbin, L.S. Wang, A study of nickel monoxide (NiO), nickel dioxide (ONiO), and Ni(O2) complex by anion photoelectron spectroscopy, J. Chem. Phys., 1 (1997) P107.

[29] A. J. Hassan, Study of Optical and Electrical Properties of nickel oxide (NiO) Thin Films Deposited by Using a Spray Pyrolysis Technique, Journal of Modern Physics, 518(2014) 52764.

[30] N. Tsuda, K. Nasu, A. Fujimori, K. Siratori, Electronic Conduction in Oxides, second ed., Springer, Berlin, 2000.

[31] P. Pramanik, S. Bhattachraya, a Chemical Method for the Deposition of nickel oxide Thin Films, J. Electrochemical. Soc., 137 (1990) 3869.

[32] [32]: R.S. Conell, D.A. Corrigan, B.R. Powell, The electrochromic properties of sputtered nickel oxide films, Solar Energy Mater Solar Cells, 1992 (25) 301-313.

[33] [33]: R. J. Powell, W. E. Spicer, Optical Properties of NiO and COO, (Physical Review B Solid State),2 (1970) 2182.

[34] H.A.E. Hagelin-Weaver, J.F. Weaver, G.B. Hoflund, G.N. Salaita, Electron energy loss spectroscopic investigation of Ni metal and NiO before and after surface reduction by Ar+ bombardment, Journal of Electron Spectroscopy and Related Phenomena, 134 (2004) 139.

[35] K.S. Lee, H.J. Koo, K.H. Ham, W.S. Ahn, Crystal Molecular Orbital Calculation of The Lanthanum nickel oxide by Means of the Micro Soft Fortran, Bull. Korean.Chem, Soc.,16 (1995) 164.

[36] S. Hüfner, T.riserer, Electronic structure of NiO, Physical Review B, 33 (1986) 7267.

[37] A.R. Williams, J. Kübler, K. Terakura, Phys. Rev. Lett, 54 (1985) 2728.

[38] R. Merlin, Electronic Structure of NiO,Phys Rev. Lett., 54 (1985) 2727.

[39] J.G. Aiken, A.G. Jordan, Electrical transport properties of single crystal nickel oxide, Journal of Physics and Chemistry of Solids, 29 (1968) 2153.

[40] H. Sato, T. Minami, S. Takata,T. Yamada," Transparent conducting p-type NiO thin films prepared by magnetron sputtering ", Thin Solid Films, vol. 236 pp.27-31, (1993).

[41] H.J. Koo, K.S. Lee, W.S. Ahn, Crystal Molecular Orbital Calculation of the Lanthanum Nickel Oxide by Means of the Micro-Soft Fortran, Bull.Korean.Chem.Soc., 16 (1995), 164.

[42] H.W. Ryu, G.P. Choi, G.J. Hong, J.S. Park, Growth and Surface Morphology of Textured NiO Thin Films Deposited by Off-Axis RF Magnetron Sputtering, Jpn.J.Appl.Phys., 43 (2004) 5524.

[43] Z. Zhiwie, Oxygen reduction lithiated nickel oxide as catalyst and catalyst support, PhD thesis case Western Reserve university, 1993.

[44] N. Benbelkacem, Synthesis and characterization of mixed complexes of cobalt (III) with ethylenediamine, a series of amino acids and nitrogen bases, memory of magister, mouloudmammeri university, Tizi-ouzou, 2012.

[45] A. Mahroug, Study of thin layers of Zinc Oxide doped Aluminum and Cobalt developed by the sol gel-spin coating technique. Application to photodetection and photocurrent, Doctoral dissertation, Université Brothers Mentouri, Constantine, 2015.

[46] Maissel, L. I., and Clang, R., (eds.), Handbook of Thin Film Technology, McGraw-Hill, New York (1970) 2. Vossen, J. L., and Kern, W., (eds.), Thin Film Processes, Academic Press, New York (1978) 3.Bunshah, R. F., (ed), Deposition Technologies for Films and Coatings: Developments and Applications, Noyes Publications, Park Ridge, NJ(1982).

[47] Cuffy, J. I., (ed.), Electrodeposition Processes, Equipment & Compositions, (Chemical Tech. Rev. No. 206), Noyes Publishing Company, Park Ridge, NJ (1982). See also; Metal Finishing '86, 54th Guidebook Directory Issue 1986, Vol. 84, No. 1A, Metals and Plastics Publications, Inc., Hackensack, NJ (1986); Durney, L. J., Electroplating Engineering Handbook, Fourth Ed., Van Nostrand Reinhold Co., New York (1984).

[48] D.S. Ginley, J. D. Perkins, Handbook of transparent conductors, Springer science, NewYork. 2010.

[49] A. Khan, Synthesis of Strontium Cuprates (Sr Cu2O) by MOCVD as a thin layer of transparent conductive oxide of type P, PhD thesis, Grenoble University, 2006.

[50] L. Tomasini (SOLLAC, Usinor Group), Surface treatments under vacuum, La Revue de Métallurgie- CIT April 2001.

[51] N. Nakamura, H. Nakagawa, K. Koshida, M. Niiya, Proceeding of the 5th International Display workshops, (1998) 511.

[52] J. A. Najim, J. M. Rozaiq, Effect Cd Doping on the Structural and Optical Properties of ZnO Thin Films, International Letters of Chemistry, Physics and Astronom, 10 (2) (2013) 137-150.

[53] https://www.researchgate.net/figure/10-Cathodic-sputtering-accelerated-Ar-ions-extract atoms-from-the-target_fig9_278637056 [accessed 16 May, 2020].

[54] D. B. Chrisey and G. K. Hubler, Plused laser deposition of thin films, John Wiley and Sons, New York (1994).

[55] http://en.wikipedia.org/wiki/Pulsed_laser_deposition (Date accessed: 13 April 2010).

[56] K.C. Sanal, Development of p-type transparent semiconducting oxides for thin film transistor applications, phd thesis, cochin university of science and technology, 2014.

[57] K. Badeker, Annalen der Physik 327, 749-66.

[58] C.M. Wang, C.Y. Wen, Y.C. Chen, K.S. Kao, D.L. Cheng, C.H. Peng, Effect of deposition temperature on the electrochromic properties of electron beam-evaporated WO3 thin films, Integrated Ferroelectrics, 158 (2014) 62-68.

[59] L. Holland, Vacuum deposition of thin films. First Edition, Published 1956 by Wiley & Sons.

[60] A.H. Rosenfeld, T. Kaarsberg, M. J. Romm, Technologies to Reduce Carbon Dioxide Emissions in the Next Decade, Phys. Today, 53 11 (2000) 29-34.

[61] J. Bellingham, R. Phillips, W. A. Adkins, Electrical and optical properties of amorphous indium oxide, J. Phys.: Condens. Matter. , 2 28 (1990) 6207.

[62] R.G. Gordon, Criteria for Choosing Transparent Conductors, Mrs Bulletin, 25 8 (2000) 52-57.

[63] A. Mahan, P. Parilla, K. Jones, A. Dillon, Hot-wire chemical vapor deposition of crystalline tungsten oxide nanoparticles at high density, Chemical physics letters, 413 (2005) 88-94.

[64] H. Hosono, M. Yasukawa, H. Kawazoe, Novel oxide amorphous semiconductor: Transparent conducting amorphous oxides. Non Cryst.Solids, 203(1996) 334-44.

[65] A.C. Pierre, Introduction to sol-gel processing, Springer Science & Business Media, 2013.

[66] S. Pawar, synthesis and characterization of Sm0.5Sr0.5CoO3 films for solid oxide fuel cell application, PhD thesis, Shivaji University Kolhapur, 2011.

[67] C. Patil, N. Tarwal, P. Shinde, H. Deshmukh, P. Patil, Synthesis of electrochromic vanadium oxide by pulsed spray pyrolysis technique and its properties, Journal of Physics D: Applied Physics, 42 (2009) 025404.

[68] A. K. Bhosale, spray deposition and characterization of cerium oxide, cerium oxide silica and cerium oxide-zirconium thin films for optically passive counter electrodes in electrochromic device, PhD thesis, Shivaji University, Kolhapur, 2009.

[69] M. A. Mahadik, , Degradation of organic impurities in water using monocrystalline ferric oxide semiconductor thin films, PhD thesis, Shivaji University, 2014.

[70] P. S. Patil, Versatility of chemical spry pyrolysis technique, Material Chemistry and Physics vol. p.59, (1999).

[71] G. Slewah, Study of Electrical and Optical Properties of Thin Film of CdS and CdS: In Prepared By Spray Pyrolysis Technology, M.Sc. Thesis, College of Sciences, University of Basrah, (1990).

[72] www.cdhfinechemical.com

[73] I. Labdaoui «Elaboration and characterization of thin films of transparent and conductive by spray pyrolysis, Master Thesis, University of Larbi Ben M'Hidi-Oum elbouachi (2013).

[74] www.Airbrushresourcecenter.com

[75] M. Amer Hassan, The effect of the annealing and annealing processes on some physical properties of the Cu2S film prepared by the method of pyrolysis, Master Thesis, University of Technology, Department of Applied Sciences (2002).

[76] A. Mahjoub, course in characterization techniques.

[77] G. Huertas, Doctoral thesis, University of Bordeaux I (2006).

[78] L. Chinnappa, investigation of the effects of certain crucial process parameters on the solar cell related optical and electrical properties of doped tin oxide films fabricated using a low cost spray technique, PhD thesis, Bharathidasan University, 2012.

[79] M. Thomson, The Modification of Thin Film Surface Structure via Low Temperature Atmospheric Pressure CVD Post Process Treatment Material, Doctoral Thesis, Salford Greater Manchester University, United Kingdom, (2013).

[80] N. M. Pinto Neves, Al-doped ZnO ceramic sputtering targets based on monocrystalline powders produced by emulsion detonation synthesis – deposition and application as a transparent conductive oxide material, PhD thesis, Nova Liboa University, 2015.

[81] JCPDS cards of NiO (Joint Committee on Powder Diffraction Standards)

[82] A J. Ragina, Preparation and characterization of tin based semiconducting thin films, PhD thesis, Kannur University, 2012.

[83] R. K. Al-Hakim, Adel KhudairHussain, The Foundations of Electronic Engineering, Ministry of Higher Education Press, Baghdad (1980).

[84] S A. Vanalakar, chemical synthesis of cds, ZnO and CdS sensitized ZnO thin films and their characterization for photo-electrochemical solar cells, PhD thesis, Shivaji University, Kolhapur, 2010.

[85] S. Benhamida, Characterization of Thin Films of nickel oxide (NiO) Elaoré by Spray Pyrolysis, Doctoral Thesis, Biskra University, Algeria, (2018).

[86] P. Sharma, An optical study of chalcogenide glasses using Uv-Visible-Nir spectroscopy, PhD thesis, Jaypee University, 2015.

[87] H. PisalSunanda, Studies on chemical routes for fictionalization of carbon annotates and their physic chemical characterization, PhD thesis, Bharati Vidyapeeth Deemed University, 2015.

[88] A. Tabet, Optimization of production conditions (substrate temperature and distance beak substrate) thin films of ZnO by spray, memory of magister, university Mohamed Khider, Biskra, 2013.

[89] M. Rezvani, L. Farahinia, structure and optical band gap study of transparent oxfluoride glass ceramics containing CaF2 nano crystals Materials & Design, 88 (2015) 252-257.

[90] R. Noui, Characterization thin layers of NiO: Cu developed by the pneumatic spray technique, Master thesis, Biskra, 2018.

[91] Perloff, D. S., Gan, J. N., and Wahl, F. E., Dose Accuracy and Doping Uniformity of Ion Implantation Equipment, Solid State Tech., 24(2) (1981).

[92] R. Ueda, J. B. Millin, Crystal Growth and Characterization, Mc Grew- Hill, (1975).

[93] S. Berrouis, D. Bensefira , Elaboration et caractérisation de couche mince NiO:Co, Mémoire de Master, Université Biskra, 2018.

[94] N. A. Bakr, S. A. Salman and A. M. Shano, Effect of Co Doping on Structural and Optical Properties of NiO Thin Films Prepared By Chemical Spray Pyrolysis Method, International Letters of Chemistry, Physics and Astronomy, 41, pp 15-30, 2014.